NRC·CNRC Aerospace

Review of Aeronautical Fatigue and Structural Integrity Work in Canada (2023 – 2025)

Editor: Dr. Min Liao

Report No.: LTR-SMM-2025-0058
RDIMS No.: N/A
Date: March 28th, 2025

National Research Council Canada | Conseil national de recherches Canada

Canada

NATIONAL RESEARCH COUNCIL CANADA (NRC)

AEROSPACE

Review of Aeronautical Fatigue and Structural Integrity Work in Canada (2023 – 2025)

Volume 1 of 1

Report No.: LTR-SMM-2025-0058

RDIMS No.: N/A

Date: March 28th, 2025

Editor: Dr. Min Liao

Classification:	Unclassified	Distribution:	Unlimited
For:	International Committee on Aeronautical Fatigue and Structural Integrity (ICAF)		
Reference:	-		
Submitted by:	Dr. Rick Kearsey, Director, Structures and Materials Performance Laboratory		
Approved by:	Dr. Mouhab Meshreki, Director in General, Aerospace Research Center		

Pages:	56	Copy No.:	N/A
Figures:	37	Tables:	4

EXECUTIVE SUMMARY

This report provides a review of aeronautical fatigue and structural integrity work carried out in Canada during the period from April 2023 to March 2025. The review is a collection of multiple work summaries that were provided by Canadian industrial partners, universities, and government organizations. Many aspects of structural integrity, especially fatigue related work, including: full-scale testing with environmental effects, aircraft structural integrity program and fleet management, life assessment and enhancement, load and usage monitoring, structural health monitoring, non-destructive inspection, and new material and manufacturing, are covered in this report.

This national review will be presented at the *39th Conference and 32nd Symposium of the International Committee on Aeronautical Fatigue and Structural Integrity* (https://www.icaf2025.com/) on 9 -12 June 2025, Xi'an, China. The whole report will be archived on the ICAF permanent website (https://www.icaf.aero/index.php).

The page is left blank intentionally

TABLE OF CONTENTS

LIST OF FIGURES

LIST OF TABLES

1.0 INTRODUCTION

As a part of the National Review for the International Committee on Aeronautical Fatigue and Structural Integrity (ICAF), Canadian industrial partners, universities and government organizations were solicited for information describing their fatigue and structural integrity related activities over the period from April 2023 to March 2025. This review covers work performed or being performed by the following organizations:

- L3Harris - Military Aircraft Services (MAS)
- Royal Military College of Canada (RMC)
- Carleton University (CU)
- Department of National Defence (DND)
    - Defence Research and Development Canada (DRDC)
    - Directorate of Technical Airworthiness and Engineering Support (DTAES)
    - Quality Engineering Test Establishment (QETE)
    - Royal Canadian Air Force (RCAF)
- National Research Council of Canada (NRC)
    - Aerospace Research Centre (NRC Aerospace)
    - Digital Technology Research Center (DTRC)

Names of contributors (where available) and their organizations are included in the text of this review. The full addresses of the contributors are available through the ICAF Canadian National Delegate whose contact is at the end of this section.

For ease of reading, this review report is organised based on the following main topics:

- Full-Scale Structural and Component Testing;
- Aircraft Structural Integrity Program and Fleet Management;
- Fatigue Life Assessment and Enhancement Technologies;
- Load, Usage, and Structural Health Monitoring;
- Non-Destructive Evaluation;
- Fatigue and Structural Integrity of Composite; and
- Fatigue and Structure Integrity of New Materials.

References are provided after each individual work summary. For questions on this report, you may contact the individual contributor and/or the Canadian National Delegate at:

Dr. Min Liao, Principal Research Officer
Group Leader - Structural Integrity
Aerospace, National Research Council Canada
1200 Montreal Road, Building M14
Ottawa, ON, K1A 0R6, Canada
Email: Min.Liao@nrc-cnrc.gc.ca

2.0 FULL-SCALE STRUCTURAL AND COMPONENT TESTING

2.1 Experimental Strength and Finite Element Modeling of a Disbonded F/A-18 Hornet Inner Wing Step Lap Joint

Stephane Brunet, NRC Aerospace

The National Research Council of Canada (NRC) carried out a test campaign on a disbonded F/A-18 Hornet Inner Wing Step Lap Joint (IWSLJ) in collaboration with the Royal Canadian Air Force, armasuisse, the United States Navy, RUAG, and L3 Harris.

Many disbonds have been reported by the F/A-18 Hornet fleet operators. The majority of those are small relative to the size of the IWSLJ. The immediate effects of those disbonds and their changes in a long term are not well understood. As such, the NRC was tasked to conduct a component test aimed to better understand the effects of a partially disbonded IWSLJ on the F/A-18 wing structural integrity, with potentially disbond growth data and residual strength evaluation. This test campaign was completed in 2024 and follow-on finite element modelling projects are carried out, aiming at developing a representative digital twin model of this complex, hybrid lap joint.

2.1.1 DAMAGE GROWTH THROUGH CONSTANT AMPLITUDE LOADING

The fatigue cycling phase consisted of low cycle count constant amplitude loading, between +77.3% Design Limit Load (DLL) and -7.1% DLL of a representative load case. This amplitude was subsequently incremented by 5% two times during this phase. Although the amount of fatigue cycles needed to be increased significantly, this test successfully induced growth of the existing disbond. Growth was tracked at regular intervals using automated ultrasonic testing (Armanda, by the Quality Engineering Test Establishment (QETE) of DND). Figure 2 and Figure 3 show the disbond prior and at the end of the test campaign, respectively. The disbond mainly grew in the chordwise direction, but also in the spanwise direction, no further than the second step, where a row of fasteners attaches the kick rib to the lower skin.

2.1.2 RESIDUAL STRENGTH

Residual strength testing (RST) was successfully completed, after applying two static cases, one up-bending at 136.8% DLL and one down-bending at 153.6% DLL, considering environmental factors. This showed that the test article was able to withstand RST static loads with no catastrophic failure of the structure, even with the larger disbond.

2.1.3 OUTCOMES OF THE EXTENSIVE INSTRUMENTATION SETUP

The test article was instrumented using traditional strain gauges (38 rosettes and 144 uniaxial gauges), mostly in the area of the step lap joints, on both upper and lower skins. Multiple optical

fibres were also bonded to the upper and lower skins to continuously record strain data along the spars and wing root lugs. A digital image correlation (DIC) setup was also used to record a strain field in the area of the lower skin step lap joint. The data collected through these three methods showed that the load distribution did not change overall, although some local effects (i.e., strain change) in the vicinity of the disbond were captured with digital image correlation (Figure 4).

A novel method for measuring the disbond size and then its growth was developed using the digital image correlation data. NRC plans to pursue the work on this subject, more specifically to assess the accuracy of the method, using the inspection data as a reference.

2.1.4 STEP-LAP JOINT FINITE ELEMENT MODELLING

Two three-dimensional finite element models were developed (more detail in Section 7.1), with and without the adhesive explicitly modelled, in order to compare results of multiple disbond configurations using various composite fracture models (Cohesive Zone Modelling – CZM, Virtual Crack-Closure Technique – VCCT) with analysis and test results from the Defence Science and Technology Group (DSTG) (Figure 5). Table 1 shows that the NRC VCCT modeling including IM7 fracture gave close results to the DSTG test. The current effort is to reproduce the actual step lap joint configuration of the test article lower skin in order to obtain a representative digital twin model of the joint for further damage growth simulation and residual strength assessments, with different disbond damages.

All testing was carried out at the Structural Integrity Laboratory, Building M-14, NRC Aerospace Research Centre, Montreal Road Campus in Ottawa, Ontario, Canada. The test started in July 2022 and was completed in January 2024.

Figure 1: Test article and test setup

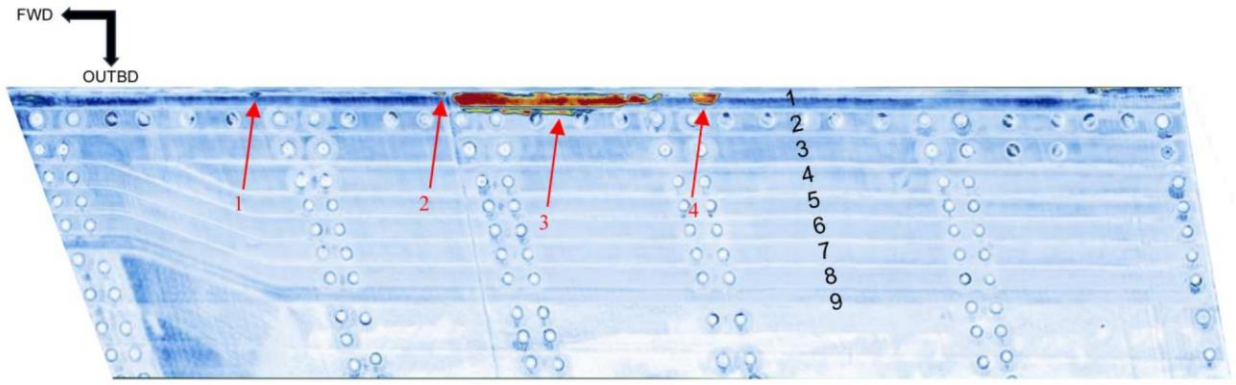

Figure 2: Baseline inspection showing initial disbond on test article lower step lap joint

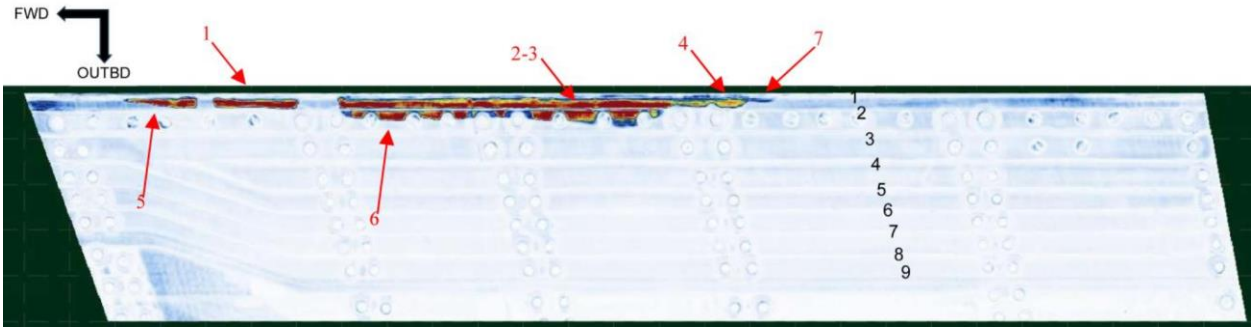

Figure 3: Final inspection showing disbond growth on test article lower step lap joint

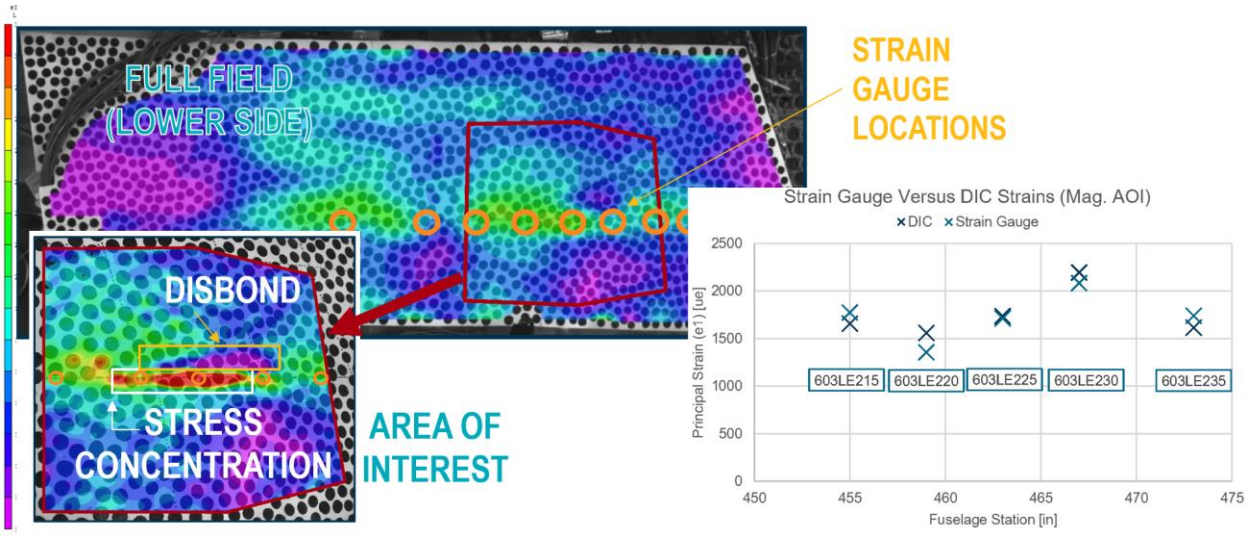

Figure 4: Digital image correlation strain map showing local effects of the disbond

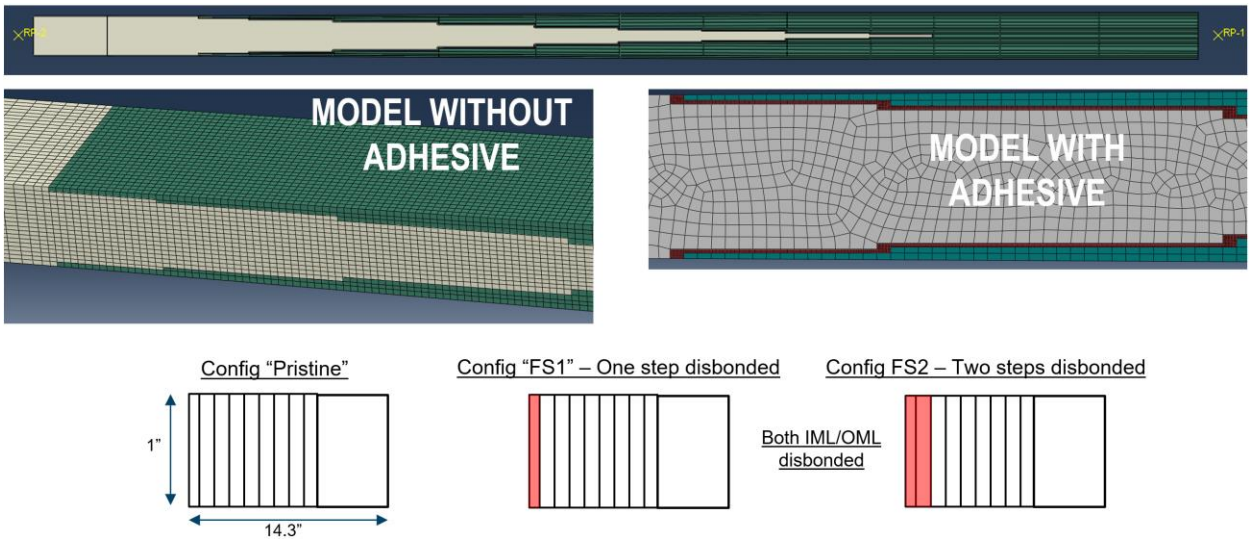

Figure 5: NRC Finite Element Models

Table 1: Comparison of Finite Element Modelling results (Failure load)

Config	DSTG (Converted Results - kN)		NRC Finite-Element Modelling (kN)			
	Test	CZM	Adhesive-centre	VCCT (adhesive fracture)	VCCT (IM7 fracture)	CZM (IM7 fracture)
Pristine		216	271	345	161	184
FS1		183	205	265	125	121
FS2	**93.1**	118	135	190	93	79

2.1.5 REFERENCES

[1] Dionne, E, Backman, D., Beltempo, A., Brunet, S., and Bolduc, B., Experimental Strength and Fatigue Assessment of a Disbonded F/A-18A/B/C/D Inner Wing Step Lap Joint, Proceedings of the 31st Symposium of the International Committee on Aeronautical Fatigue and Structural Integrity (ICAF2023), 26 – 29 June 2023, Delft, The Netherlands.

[2] Brunet, Stéphane, Backman, Dave, Li, Gang, Renaud, Guillaume, Liao, Min, "On the testing of F/A-18 Hornet Inner Wing Step Lap Joints", The 40th Aircraft Structural Integrity Program Conference, Austin TX, 12/2/2024-12/5/2024, CPR-SMM-2024-0191, 2024-11-08.

3.0 AIRCRAFT STRUCTURAL INTEGRITY PROGRAM AND FLEET MANAGEMENT

3.1 CF-188 Aircraft Structural Integrity Program (ASIP)

L3Harris - Military Aircraft Services (MAS)

L3Harris MAS, a wholly owned subsidiary of L3Harris, is among Canada's leading In-Service Support (ISS) integrator, offering military and commercial customers a full range of modifications and sustainment solutions, in support of their aircraft fleets. L3 MAS employs over a thousand people in its main facility in Mirabel, Quebec and in other operating centers throughout Canada (Bagotville, Cold Lake, Halifax, Shearwater, Comox, Pat Bay, Greenwood, Gatineau, Ottawa, Toronto, Trenton and Petawawa).

L3Harris MAS provides ISS services to the Royal Canadian Air Force (RCAF) on the following platforms:

- CF-188 Hornet
- CT-114 Tutor
- CH-148 Cyclone
- CC-150 Polaris
- CC-330 Husky
- CP-140 Aurora

3.1.1 CF188 HORNET - AIRCRAFT STRUCTURAL INTEGRITY PROGRAM (ASIP) AND LIFE EXTENSION PROGRAM (ALEX)

Since 1986, L3Harris MAS performs the in-service support of the RCAF CF-188 Hornet (Boeing F/A-18) fleet as part of System Engineering Support Contract (SESC). This contract includes the conduct of all aspects of the Aircraft Structural Integrity Program (ASIP) and of related depot level structural maintenance and fleet management activities.

3.1.2 INNER WING MOTIVE FLOW TUBE CRACKING REPAIR

The RCAF had suffered repetitive cracking of an internal fuel tube in the inner wing (Figure 6). Up until now, the repair involved removing the inner wing and then the upper skin to perform a replacement of the fuel tube; this was obviously a costly operation. Via a Finite Element Analysis (FEA), the cause of cracking of this aluminium tube was found to be fatigue caused by repetitive fuel internal pressure application and deformation of the tube due to inadequate supports. The presence of a weld at the hot spot also contributed to accelerate the cracking. To avoid the costly wing-off repair, a new in-situ repair is being developed involving for the first time on the CF-188 the use of a Titanium Additive Manufactured (AM) tube to replace the cracked section (Figure 6).

The new tube section will be certified both in static and fatigue while the manufacturing aspects will be closely monitored to ensure the integrity of the AM (additive manufacturing) parts to meet the design objectives. The repair has just passed the preliminary design stage at this time.

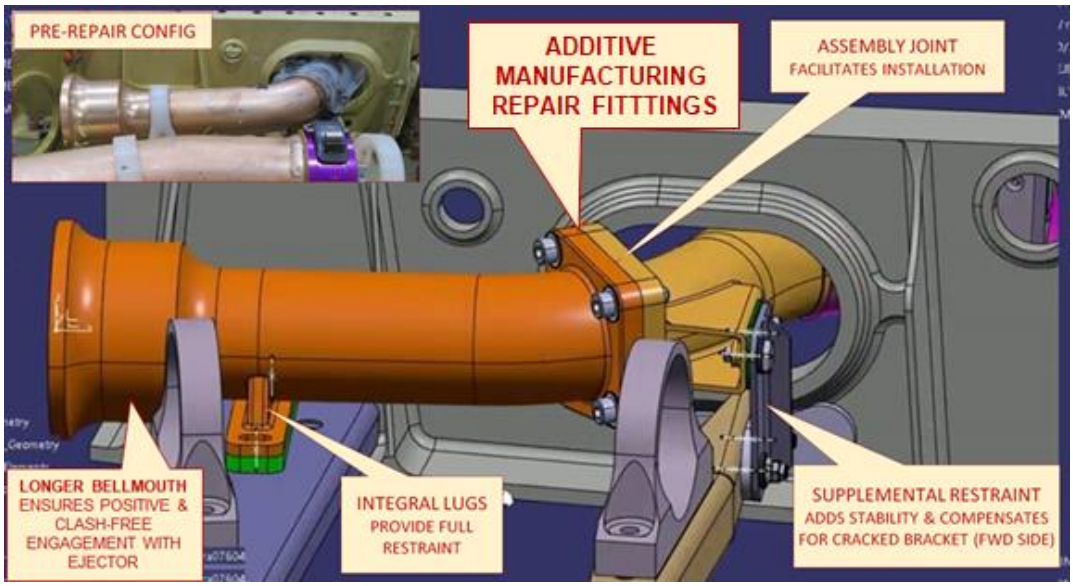

Figure 6: Proposed Repair Configuration

3.1.3 BENEFIT OF FLEET SUNDOWN TO PERFORM AGE EXPLORATION INSPECTIONS

The RCAF fleet has reached a point where some fleet leaders start to retire as they reach their life limits. Upon retirement, these aircraft are being dismantled to retrieve still serviceable parts providing access to structural parts normally not accessible under a regular maintenance program. The opportunity is therefore taken to deploy an Aircraft Sampling Inspection (ASI) program, as summarized in Figure 7, to meet three fatigue related objectives:

1) Validate the effect on the fatigue damage accumulation resulting from a change of fleet Baseline Operating Spectrum (BOS) (i.e., comparing analytical predictions to real in-service data).
2) Obtain fleet leaders damage condition for hot spots posing high analytical challenges as being driven by compressive usage spectrum which CG models are difficult to handle.
3) Accelerate on-going ASI tasks by getting more valuable candidate and minimising operational impacts on serviceable aircraft.

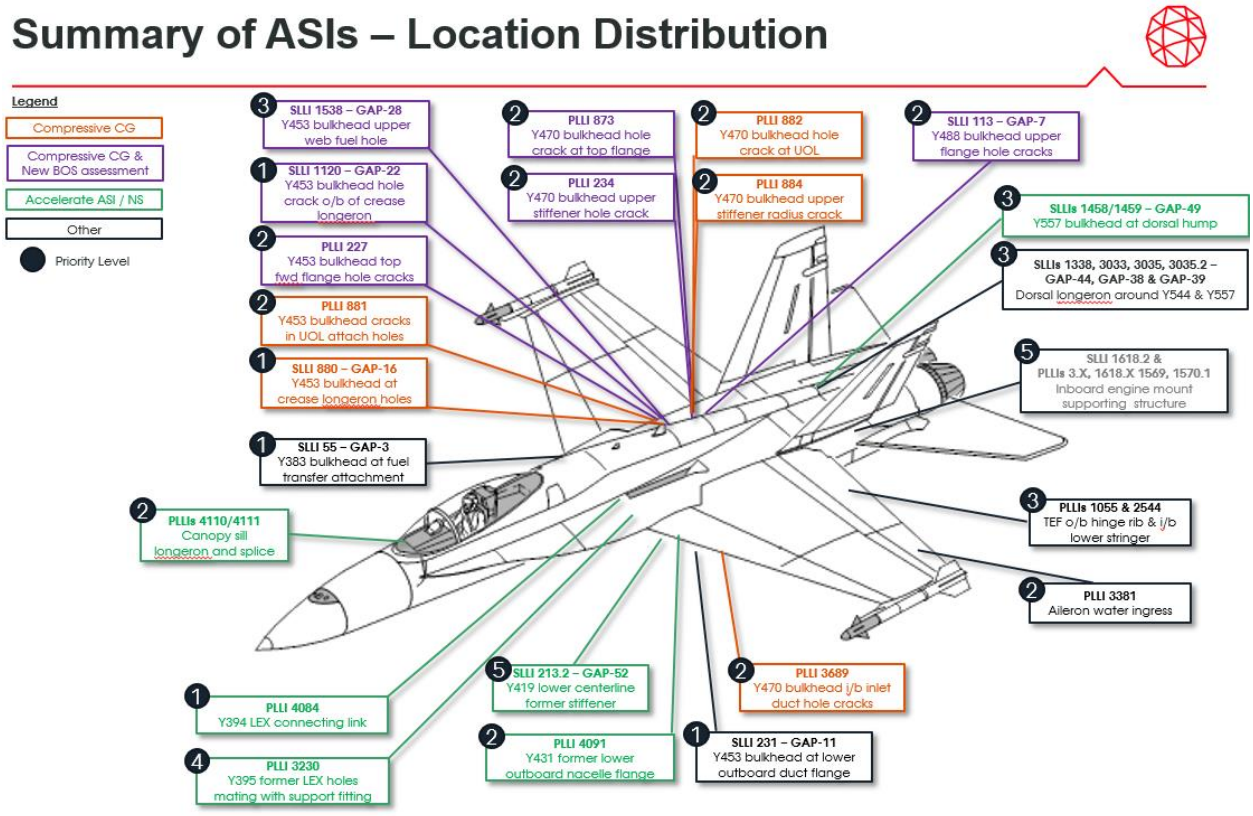

Figure 7: Sampling Locations

This program is still under development as of this writing.

3.2 CH-148 Cyclone – Aircraft Structural Integrity Program (ASIP)

As part of the Maritime Helicopter Program, L3Harris MAS is mandated to conduct an ASIP program on the CH-148 (Figure 8) by the RCAF. Usage monitoring uses raw data files collected through the Health and Usage Monitoring System (HUMS). The HUMS has the capability to recognize regimes/manoeuvres via recorded flight parameters and sensor data. This data is processed by the Usage Comparison and Reporting Tool (UCART) that computes fatigue damage rates at selected locations for each individual aircraft and compares them to the design spectrum according to the requirements of MIL-STD-1530.

Since 2021, several algorithms for fatigue damage rate derivation in UCART from the HUMS regime and event data have been corrected for improved accuracy. The control points forecasted at the early days of the program have to be changed and some others have been added. Filtering of the captured regime data was implemented in order to provide realistic usage data and avoid multiple triggering of the regime recognition when aircraft is operating close to the defined

thresholds. Additional modifications were also made to UCART to correct false ship-based taxi signal discovered during regime recognition validation. With those corrections implemented, the fleet usage was reprocessed and the fleet usage calculation is now considered steady and reliable.

The other major component of the CH-148 ASIP Program is the Structurally Significant Item (SSI) database. The SSI database records all the relevant information about each SSI, also known as Primary Structural Element (PSE), from the design phase and into the in-service phase in order to enable ASIP analysts to monitor structural defects and, when needed, recommend changes to the maintenance program or modifications to the helicopter.

Usage monitoring and structural condition monitoring are now well implemented and periodic reporting is now done, in support of the fleet management.

Figure 8 CH-148 Cyclone helicopter (https://www.canada.ca/en/department-national-defence/services/procurement/ch-148-cyclone.html)

4.0 FATIGUE LIFE ASSESSMENT AND ENHANCEMENT TECHNOLOGIES

4.1 Airframe Digital Twin Technology Development and Demonstration

Yan Bombardier, Guillaume Renaud, Min Liao, NRC Aerospace

The National Research council of Canada (NRC) developed an Airframe Digital Twin (ADT) framework to support aircraft sustainment based on the damage tolerance approach. The primary objective of this framework is to enhance the accuracy of structural diagnosis and prognosis to allow better maintenance decisions. The framework integrates cutting-edge structural analyses including high-fidelity finite element simulations, probabilistic modelling techniques including advanced probabilistic crack growth modelling and quantitative risk assessments. The framework also provides the capability to periodically update the probabilistic inputs of these models as new data about the airframe becomes available, such as inspection results, usage, and other relevant factors.

NRC's ADT framework was used to simulate the CF-188 aircraft inboard leading edge flap (ILEF) durability and damage tolerance fatigue test, referred to as FT382. A digital twin of the CF-188 ILEF attachment lugs was developed to demonstrate the ADT framework, perform sensitivity studies, and assess the potential benefits of using digital twin concepts for lifing and sustainment of airframe structures. This work was presented at ICAF 2023 [3]. More recently, two new modelling aspects were included in the ADT framework and demonstrated for the CF-188 ILEF: a) the calculation of hazard rate (HR) and cumulative probability of failure (CPOF) using conditional probability of failure equations, and b) the effect of local load uncertainty on the resulting HR and CPOF. The final results were published by Bombardier et al. in 2024 [4].

Compared to conventional lifing methods, the CF-188 ILEF attachment lugs demonstrator showed that the ADT approach has the potential to extend the time to the first inspection and extend the inspection intervals. Although the CF-188 ILEF attachment lugs may not be the best candidate for demonstrating a crack growth modeling based ADT framework, NRC demonstrated that:

1) The load tracking factor could be reduced from 1.50 to 1.36, resulting in +10% life extension.
2) The time to the first inspection could be increased by up to 47% from the point of acceptable limit (PAL) calculated using the CF-188 Lifing Policy, for a scenario of 1% of the cracks nucleated from surface scratches and 99% of the cracks nucleated from the equivalent pre-crack size (EPS)at time zero.
3) The repeated inspection interval could be increased by up to 230%, compared to the inspection interval for safety by inspection (SBI) calculated using the CF-188 conventional

lifing method, for a scenario of 1% of the cracks nucleated from surface scratches and 99% of the cracks nucleated from the equivalent pre-crack size (EPS) at time zero.

It was also found that the standard practices for the aircraft structural integrity program (ASIP) outlined in MIL-STD 1530D (Department of Defense, 2016) align very well with NRC's ADT framework. As such, the framework could provide a solid basis for supporting aircraft that are managed using MIL-STD 1530D.

This NRC ADT project has been reported in the previous ICAF national reviews. As this multi-year project is closed in 2024, the authors would like to acknowledge the funding provided by the Defence Research and Development Canada (DRDC) and NRC for supporting this research and development efforts. The authors would also like to acknowledge the technical support of L3Harris for providing load data, Mr. Yvan Caron and his team from the Directorate of Technical Airworthiness and Engineering Support (DTAES) for supporting and guiding the project since its inception in 2017.

4.1.1 REFERENCES

[3] Bombardier, Y., Renaud, G., & Liao, M. (2023). Development and demonstration of damage tolerance airframe digital twin methods and tools. International Committee on Aeronautical Fatigue and Structural Integrity (ICAF), Delft, The Netherlands.
Link: https://www.icaf.aero/icaf2023/proceedings/display_manuscript/24.htm

[4] Bombardier, Y., Renaud, G., & Liao, M. (2024). Development and Demonstration of a Digital Twin Analysis Framework for Airframe Life Cycle Management. 2024 Aircraft Structural Integrity Program (ASIP) Conference, Austin, Texas, United States of America.
Link: https://www.arctosmeetings.com/agenda/asip/2024/proceedings/presentations/P26257.pdf

4.2 Development of a Rotorcraft Structural Component Digital Twin

Guillaume Renaud, Zohreh Asaee, Yan Bombardier, Cathy Cheung, NRC Aerospace

Life cycle management of rotorcraft has traditionally relied on deterministic life predictions, utilizing safety factors for usage, loads, and fatigue strength. Consequently, the retirement life of helicopter structural components can be overly conservative, leading to unnecessary maintenance costs and reduced aircraft availability.

The objective of this work is to assess and adapt concepts of digital twin for structural sustainment, previously developed at the National Research Council of Canada (NRC) (see Section 4.1 and [5]), to a safe-life framework typically used to determine the retirement life of rotorcraft structural components [6]. For this implementation, the cumulative probability of failure (CPOF) and the hazard rate are computed as a function of elapsed time using a probabilistic stress-life (S-N) model and uncertain individual component loads. These loads are inferred using a machine learning (ML)

model that correlates component loads with flight state and control system parameters, without relying on maneuver or usage recognition. The feasibility and applicability of this approach are currently under evaluation for a structural component of the CH-146 Griffon helicopter operated by the Royal Canadian Air Force (RCAF) [7].

4.2.1 MATERIAL MODEL

A probabilistic S-N model was developed by fitting available test results. The resulting model includes a parameter (endurance limit) that is normally distributed. This model captures the uncertainty in material data due to scatter and limited test results. It is illustrated in Figure 9a).

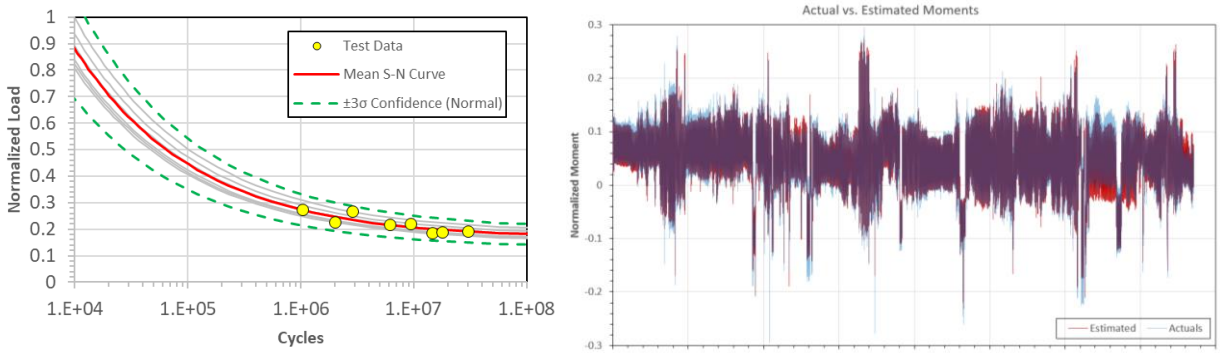

a) Probabilistic S-N Model b) Example of estimated loads using ML model

Figure 9: Probabilistic S-N model and example of load estimation.

4.2.2 LOADS MODEL

Instrumented flight data were used to train a ML model that estimates the component structural loads from a number of selected flight state and control system parameters. Multiple approaches for flight data processing and machine learning were implemented and a few candidate models were retained. The loads estimated from one of these models are shown in Figure 9 b), along with the measured loads of flights that were not used for ML training (ML testing). To capture the uncertainty in the ML model, a load estimation error model was developed using the ML testing flight data. The probabilistic load estimation model was therefore obtained by superposing the loads estimated using ML (deterministic) and the load estimation error model (probabilistic).

4.2.3 QUANTITATIVE RISK ASSESSMENT

Parametric studies were carried out to evaluate the relative effect of different types of uncertainties on risk assessment metrics. A comparison of the "safe" life to a CPOF of 1E-06 is presented in Table 2, and the probability density functions of the full life distributions, are presented in **Error!**

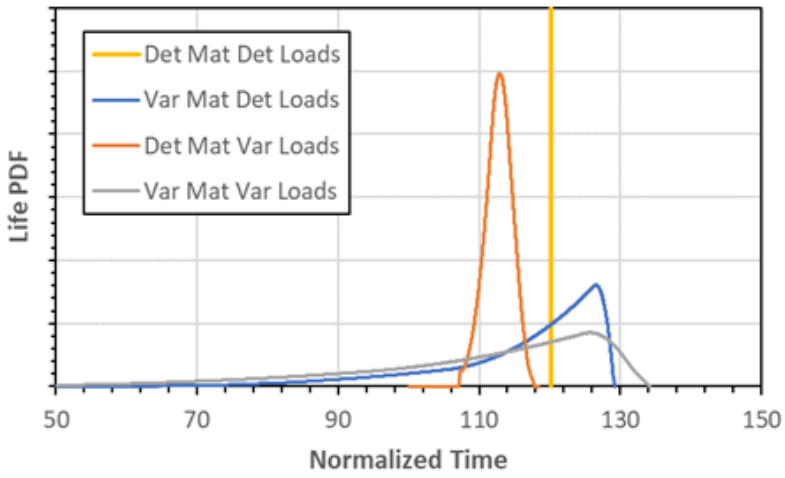

Reference source not found..

The labels "Det" and "Var" correspond to deterministic (median) and probabilistic analyses, applied to the material ("Mat") or the loads. The results show that, for this specific problem and using this specific ML model, the "safe" life to a CPOF of 1E-06 is approximately 6 times the current component retirement life, if all uncertainties are considered and modeled. Moreover, the median life is over 120 times the current component retirement life.

Table 2: Sensitivity Study Safe Life Results

Study	Normalized Life*	
	Median	CPOF = 1E-06
Det mat Det Loads	120.22	-
Var Mat Det Loads	119.53	9.02
Det Mat Var Loads	112.84	102.20
Var Mat Var Loads	112.81	5.96

* Life divided by current component life limit

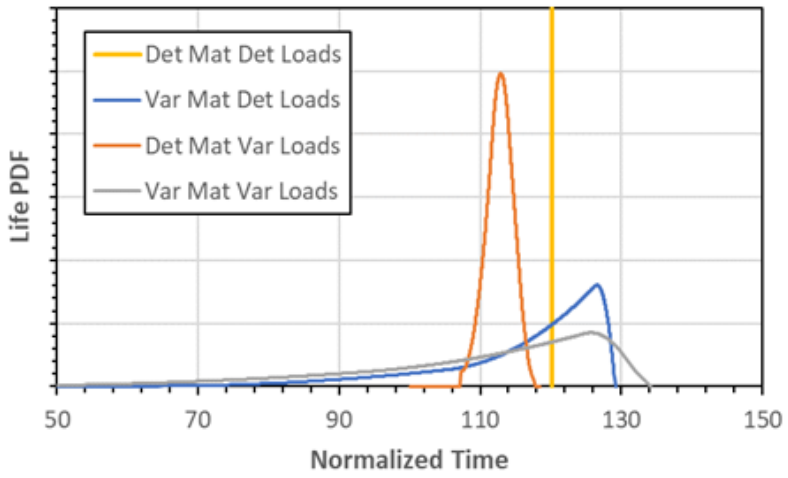

Figure 10: Sensitivity Study Life Probability Density Function (PDF) Results.

4.2.4 REFERENCES

[5] Renaud, G., Bombardier, Y. , Liao, M., "Development and Demonstration of a Digital Twin Analysis Framework for Airframe Life Extension," NATO AVT-369 Research Symposium on Digital Twin Technology Development and Application for Tri Service Platforms and Systems, Båstad, Sweden, October 2023.

[6] Dickson, B., *et al.*, "Rotorcraft Fatigue and Damage Tolerance," 25th European Rotorcraft Forum, Rome, Italy, September 1999.

[7] Asaee, Z., Renaud, G., Bombardier, Y., Cheung, C., "Integration of Machine Learning and Probabilistic Methods for Structural Life Assessment in Helicopter Digital Twins," Vertical Flight Society's 81st Annual Forum, Virginia Beach, USA, May 2025.

4.3 Development of Stress Intensity Factor Solutions for a Radial Crack at a Hole Filled with Neat Fit and Interference Fit Fastener

Yan Bombardier, NRC Aerospace

Safe life and damage tolerance analyses are typically conducted by assuming that a crack nucleates and grows from an open hole. Filling the hole with a fastener or a bushing changes the load distribution and can positively affect the predicted fatigue life. The resulting effect depends on the loads (type, magnitude, and orientation), materials, dimensions, and tolerances. To the knowledge of the author, no comprehensive stress intensity factor solution existed for radial cracks at filled hole when this research project was initiated in 2020. Based on this premise, the National Research Council of Canada (NRC) developed new stress intensity factor solutions in an attempt to improve the accuracy of crack growth simulations for radial through fatigue cracks growing from holes filled with fasteners. The objectives of this research project are:

1) To develop stress intensity factor solutions that consider the presence of fasteners in holes;
2) To develop tools and methodologies to integrate these new solutions with commonly used crack growth software, e.g. AFGROW;
3) To demonstrate analytically the effect of filled holes on crack growth lives; and
4) To compare analytical predictions to experimental results, if available.

The cracking scenario that was analysed consists of a radial through crack nucleating and growing from an offset hole that is filled with a neat fit or interference fit fastener. The geometry of the cracked plate is illustrated in Figure 11. Two loading conditions were modelled: remote bypass stress and pin loading.

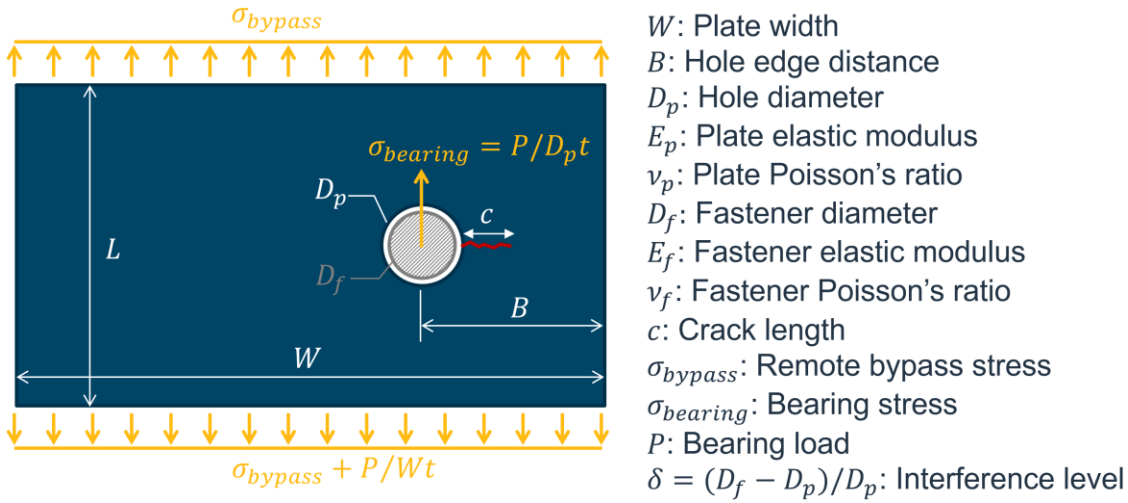

Figure 11: Radial crack growing from a hole filled with a fastener

The analysis of this problem is non-linear due to the contact between the plate and the fastener. As such, the stress intensity factor solutions were developed from finite element analyses based on a full factorial experiment involving the following parameters and levels:

1) Plate elastic modulus (E_p): Aluminium, titanium, and steel (3 levels)
2) Fastener elastic modulus (E_f): Titanium and steel (2 levels)
3) Crack size (c/D_p) (20 levels)
4) Edge distance (B/D_p) (9 levels)
5) Plate width ($W/2B$) (12 levels)
6) Interference level (D_f/D_p) (5 levels)
7) Load cases: Bypass, bearing (2 levels)

The finite element analyses were conducted using MSC/Marc supported by several in-house programs to build, run, and post-process the models and results. The completion of the full factorial experiment necessitated more than 150,000 finite element analyses and several months of computation. The finite element results were extracted and fitted to an idealized mathematical model to facilitate data storage and usage for crack growth simulations. For a given geometry and crack size, the resulting stress intensity factor response varies non-linearly as a function of the applied stress, as opposed to conventional stress intensity factor solutions that vary linearly as a function of the applied stress. An example of stress intensity factors as a function of the remote bypass stress is presented in Figure 12 for several crack sizes. As shown, the stress intensity factor response is bilinear as a function of the applied remote bypass stress. The bilinearity is caused by the transition of the contact zone from a full contact between the plate and fastener due to the interference fit to a partial contact as the remote bypass stress pulls on the plate and creates a growing gap between the fastener and the plate as the stress increases.

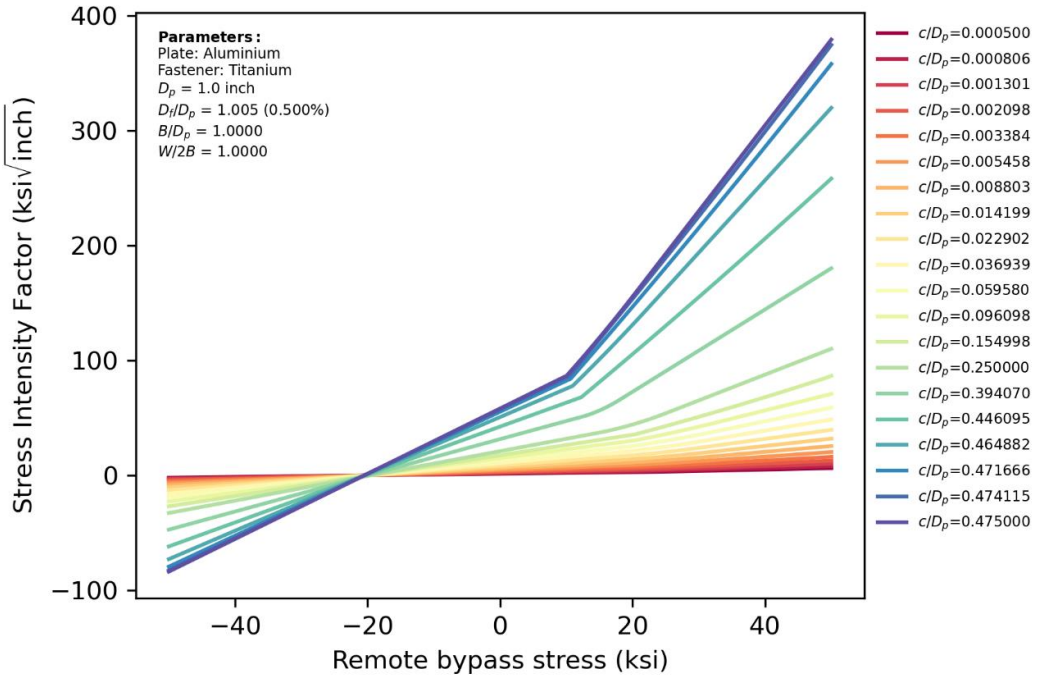

Figure 12: Example of stress intensity factor responses as a function of remote bypass stress for several crack sizes.

Due to the stress intensity factor non-linearity, common crack growth software cannot be used directly. For variable amplitude loading, the minimum and maximum stress intensity factors need to be calculated on a cycle-by-cycle basis using the crack size, as well as the minimum and maximum stresses. To facilitate the usage of the new stress intensity factor solutions, NRC developed a plugin for AFGROW that allows this process. The AFGROW plugin interface developed by NRC is presented in Figure 13.

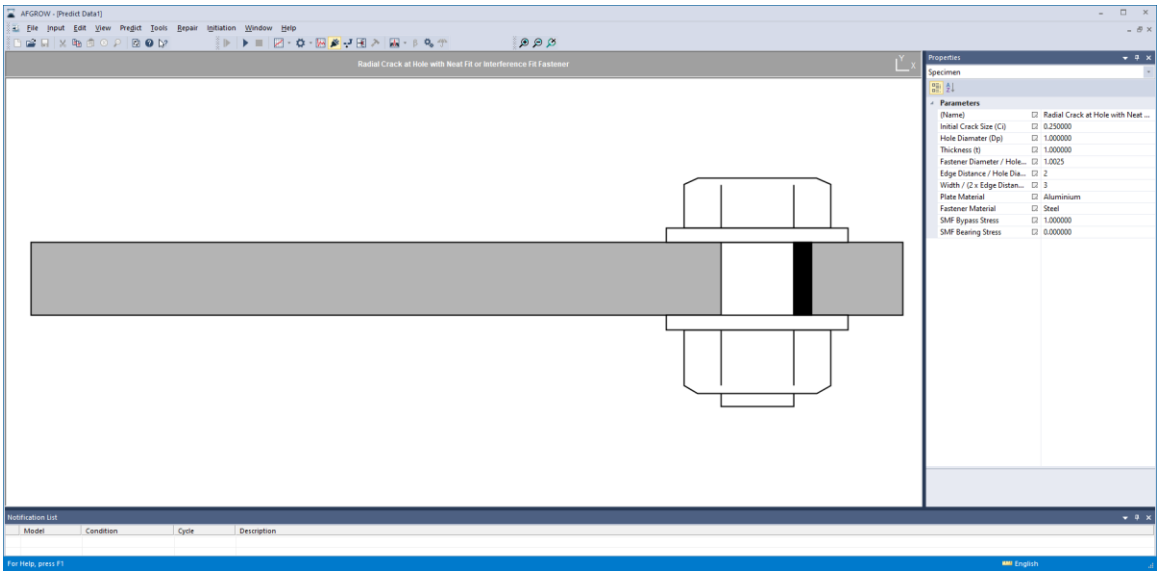

Figure 13: AFGROW Plugin for the simulation of radial cracks at filled hole.

NRC conducted several crack growth simulations using generic cases to quantify the effect of the filled holes. This was done by comparing the crack growth lives resulting from the filled hole models to the crack growth lives from open hole models. The simulations were conducted using the TWIST remote bypass stress spectra for three stress scaling factors. For the tested geometries, the predicted crack growth lives obtained by including the filled hole effect from a 0.127 mm (0.005 inch) radial crack to failure were 2 to 16 times longer than crack growth lives obtained using the open hole model. The effect of modelling the fastener on crack growth depends on the geometry, interference fit level, and applied loading. For all tested scenarios, the presence of the fastener inside the hole extended the predicted crack growth lives by at least two times compared to the open hole assumption.

While NRC achieved a major milestone by developing new stress intensity factor solutions and an AFGROW plugin to use these solutions, it is recognized that more work needs to be done to finalized the stress intensity factor solutions and to provide sufficient confidence in their use to accurately predict crack growth lives of structures with radial cracks filled with neat fit or interference fit fasteners. In the coming year, NRC is planning to:

1) Validate the crack growth predictions with experimental results.
2) Assess and implement superposition methods for combining the bypass and pin loading stress intensity factor solutions.
3) Evaluate and implement interpolation methods to allow arbitrary parameter values instead of discrete values.

5.0 LOAD, USAGE, AND STRUCTURAL HEALTH MONITORING

5.1 Helicopter Load and Usage Monitoring Research in 2023-2025

Catherine Cheung, NRC Aerospace

5.1.1 HELICOPTER LOAD ESTIMATION

The use of machine-learning based technologies for a variety of health and usage monitoring systems (HUMS) applications has become quite common place in recent years, such as in the topics of regime recognition, load estimation and fault detection in bearings and gears. Because there are so many different machine learning algorithms and architectures that could be employed, the potential number of solutions is vast. The amount of effort that could be devoted to training the best solution for an application could be unlimited. However, there are important analyses that could be completed upfront to expedite finding well performing models.

Ongoing efforts at NRC-AERO-SMPL to develop helicopter load estimation models using a variety of machine learning algorithms have generated promising results. As inputs, these models only use data from existing aircraft instrumentation monitoring standard flight state and control system parameters. As aircraft platforms are being flown in expanded roles than originally intended, and pressures mount to postpone aircraft retirement or replacement, operators must closely monitor the usage of the aircraft and track component loads. Digital twin frameworks (see Section 4.2, and 5.1.3), for example, would integrate operational loads and usage data of each aircraft with other tools and analyses to improve structural life prediction and fleet management capability.

In this work, several approaches to further improve machine learning models for load estimation are explored by making use of the Gamma test as well as feature selection techniques to optimize the input parameter set used for modeling. These steps can be taken before attempts to train and develop models. By attaining an indication of the best achievable model performance for the data, as well as identifying and understanding the key input parameters, this knowledge helps us to better understand the data and the output, even if the model itself is a black box. A comparison of Gamma test values using a variety of feature selection techniques is shown in Figure 14.

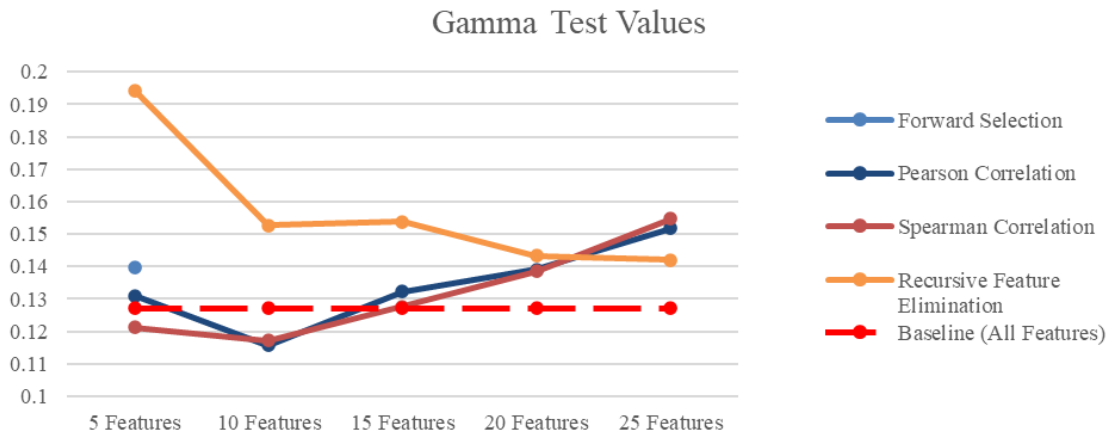

Figure 14: Comparison of Gamma test values for different feature selection methods.

5.1.2 REFERENCES

[8] C. Cheung, N. Fenev, J.J. Valdés, "Feature selection and Gamma test for improved load estimation models", Proceedings of the 81st VFS Annual Forum 2025, Virginia Beach, May 2025.

5.1.3 HELICOPTER LOAD ESTIMATION INTEGRATED INTO A HELICOPTER DIGITAL TWIN

The airframe digital twin analysis framework developed at the National Research Council of Canada is being transposed to safe life applications for rotorcraft components. A probabilistic safe life prediction approach, shown in Figure 15, consisting of uncertain material property data and uncertain load spectra is used to calculate risk assessment metrics, such as the cumulative probability of failure, the hazard rate, and the average hazard rate as a function of time. A demonstration of this approach is presented for a CH-146 Griffon component, for which the uncertain loads are estimated from a model developed through machine learning (more details see Section 4.2). This preliminary assessment shows the feasibility of using digital twin concepts as a viable alternative to traditional deterministic life predictions, with the potential to reduce maintenance costs and increase aircraft availability.

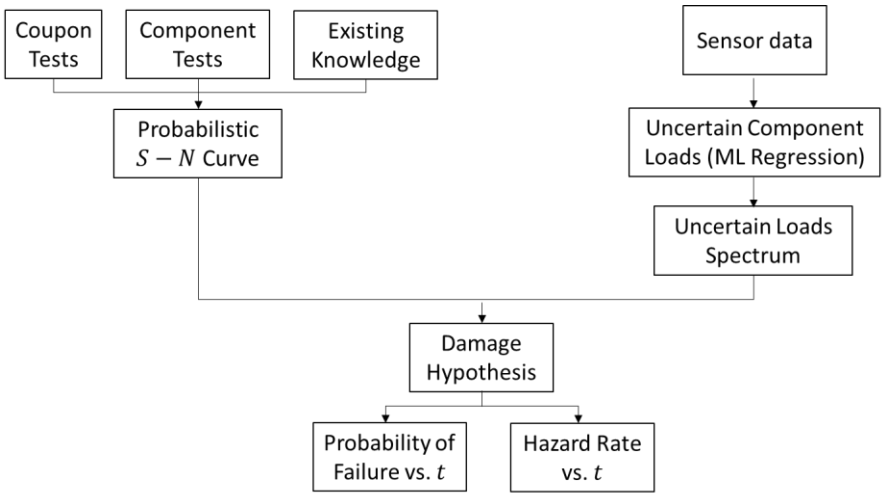

Figure 15: Probabilistic safe-life calculation approach used in NRC helicopter digital twin.

5.1.4 REFERENCES

[9] G. Renaud, Z. Asaee, C. Cheung, J. Wooldridge, "Adding Digital Twin Concepts to Helicopter Structural Component Structural Life Assessment", Proceedings of the 80th VFS Annual Forum 2024, Montreal, May 2024.

5.1.5 REGIME RECOGNITION

Regime recognition is an important tool for helicopter health and usage monitoring because it enables tracking of how the aircraft are actually flown. Their actual operational usage can then be compared to their baseline usage spectrum, and any differences in the usage can be analyzed and assessed for potential impacts to component fatigue lives, fleet operations, and maintenance. There are algorithms that exist for performing helicopter regime recognition that rely on training and testing models using flight survey data, such as those based on machine learning frameworks. Supervised machine learning models are often used for regime recognition and can be very effective, generating accurate results. However, these methods depend on large amounts of labeled training data. There are often cases where large proportions of flight data are available but not usable for model training due to a lack of verified regime labels. To properly label flight test data that are otherwise unusable, an initial labeling algorithm was developed based on helicopter regime descriptions and parameter time histories. This work presents progress in the development of this labeling tool. Improvements have been made to the tool to increase its robustness, and an approach to improving and validating the tool has been developed, which increases the confidence in the assigned labels to flight test data. Additional flight data formats are now accommodated, specifically, flight data recorder (FDR) file formats. The approach makes use of the measured position parameters and assigned labels to plot labeled flight paths in keyhole markup language (KML) format for three-dimensional visualization, shown in Figure 16. As with the previous iteration of this tool, the algorithm for labeling FDR data requires further development, but the

current results are promising, and the 3D visualization using KML files enables further improvements by highlighting which regimes require more attention for labeling.

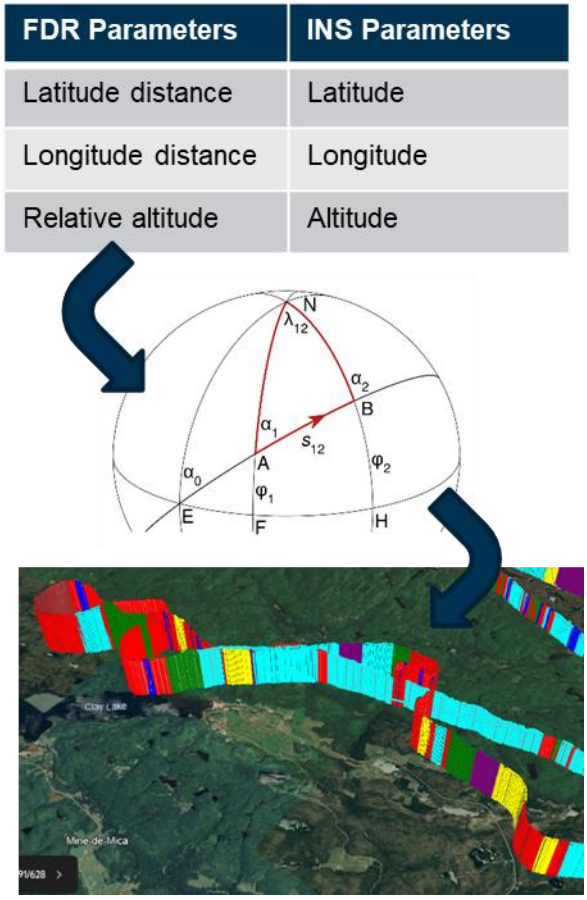

Figure 16: Converting FDR or INS parameter data to a flight path with marked regimes.

5.1.6 REFERENCES

[10] J. Wooldridge, C. Cheung, "Improving flight data labeling for regime recognition through 3-D visualization", 27th CASI Aerospace Structures & Materials Symposium, Ottawa, Nov 2023.

[11] C. Cheung, E. Seabrook, "Towards an Evaluation Process for Regime Recognition Approaches: Addressing Variability in Labeling Training Data" in *Proceedings of the Vertical Flight Society 79th Annual Forum*, West Palm Beach, FL, USA, May 2023.

5.1.7 SAE AEROSPACE STANDARD AS7140: COMMON, OPEN DATA EXCHANGE FORMAT FOR ROTORCRAFT HEALTH AND USAGE MONITORING SYSTEMS (CODEX-HUMS)

The Society of Automotive Engineers (SAE) HM-1R committee was formed with the initial intent of developing a standard data format for rotorcraft health and usage monitoring systems produced or used by an on-board or off-board system in both commercial and military applications. A

Common Open Data Exchange format for rotorcraft Health and Usage Monitoring Systems (CODEX-HUMS) would offer a more affordable, capable and effective Integrated Vehicle Health Management System, Figure 17. The objective is for end users to have access to an open data format that is machine-readable and contains the necessary HUMS information and flight data to analyze events and system anomalies, as well as enable the data to be utilized in a host of other use cases. This standard, SAE Aerospace Standard AS7140), is in the final stages of preparation and is expected to be published later in 2025.

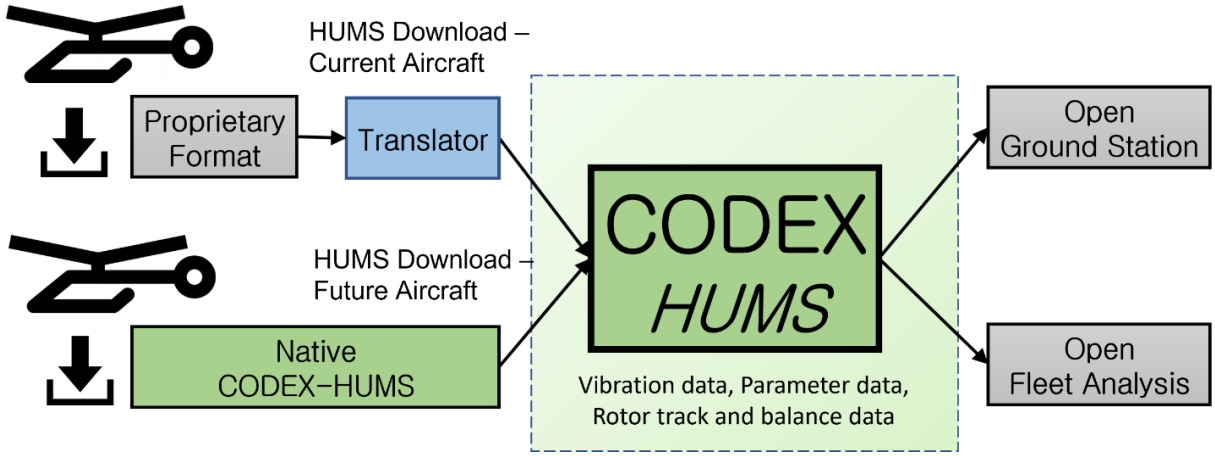

Figure 17: AS7140: Common, Open Data Exchange Format for Rotorcraft HUMS (CODEX-HUMS).

5.1.8 REFERENCES

[12] B. Tucker, C. Cheung, K.T. Royar, D. Fok, E. Carney, “Development of a Common, Open Data Exchange (CODEX) for Rotorcraft HUMS Data”, Proceedings of the 80th VFS Annual Forum 2024, Montreal, May 2024.

6.0 NON-DESTRUCTIVE EVALUATION

6.1 Detect and Characterize Impact Events in Metallic Aircraft Structure

Shashank Pant[1], Jack Wooldrige[1], Emma Seabrook[1], Julio Valdes[2], Marc Genest[1]
[1]NRC Aerospace Research Centre, NRC Digital Technologies Research Centre

Aircraft structures are vulnerable to damage from foreign object impacts, which can happen during manufacturing, maintenance, or in-service. These impacts are typically detected through observations and reports by flight or ground crews, followed by non-destructive inspection (NDI). Timely detection of such damage is crucial to ensure appropriate maintenance actions can be taken. This ongoing research at NRC aims to develop Structural Health Monitoring (SHM) methods that can automatically detect and analyze these impact events using physics-based and machine learning techniques. The focus of this summary is on the machine learning techniques.

6.1.1 EXPERIMENTAL SETUP

A cut-out from an aircraft fuselage, with dimensions of 31 by 26 inches [787.4 by 660.4 mm] and a skin thickness of 0.032 inches [0.81 mm], was used for the experiment, as shown in Figure 18. To administer impact, the metallic aircraft structure (MAS) was segmented into 1 by 1 inch [25.4 by 25.4 mm] grid patterns over an area of 22 by 20 inches [558.8 by 508 mm].

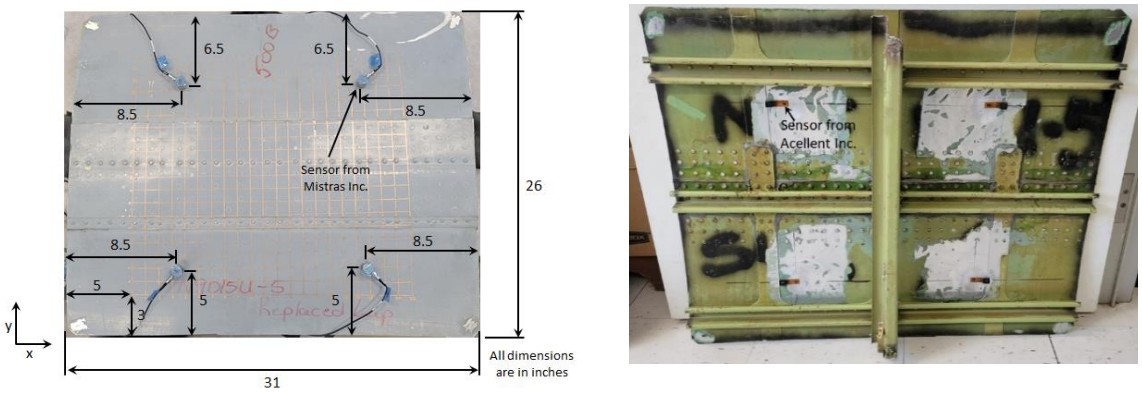

Figure 18. Metallic aircraft structure used in the experiment - dimensions in inches [x25.4 mm].

Two different sensor systems: Mistras Inc.'s acoustic emission (AE) sensors and Acellent Inc.'s lead zirconate titanate (PZT) sensors, referred to as Mis and Acl sensors, respectively, were used to collect the data. These sensors were affixed to the MAS, and were connected directly to digital oscilloscopes without any amplification or filtering. A configurable multi-use tapper with force feedback was developed to inflict impact on the test article. The tapper can be converted into a tap hammer by attaching a handle or used as a drop-weight impactor by detaching the handle.

Two sets of experiments were performed: (i) the calibration and (ii) the drop-weight impacts. In the calibration experiment, the multi-use tapper was used in the tap hammer configuration to impact each location five times with varying levels of force. In the drop-weight experiment, an additional mass of 102 grams was added to the tapper, for a total mass of 136 grams, which was dropped inside a guide-tube from four discrete heights of 100 mm, 150 mm, 200 mm, and 250 mm.

6.1.2 **ANALYSIS AND RESULTS**

A total of 48 features were extracted from the sensor signals, including time of arrival (ToA), root mean square (RMS), energy, maximum amplitude, maximum range, start and end times of the maximum range, time delay, peak frequency, frequency centroid, etc. A Gamma study was conducted using these features. The Gamma test results, with V_{ratios} for positions below 0.08 and impulse energy below 0.14, suggested that these extracted features could effectively predict impact position and impulse energy. A Permutation Feature Importance (PFI) study further assessed the importance of these features, revealing that ToA was the most crucial for position prediction, while RMS was the most significant feature for predicting impulse energy.

Two machine learning models, Random Forest (RF) and Gradient Boosting (GB), were used to predict the position, while Multi-Layer Perceptron (MLP), Support Vector Machine (SVM), and GB were utilized for predicting impulse energy. The top results for impact position prediction came from a hyperparameter-tuned GB model trained on Mis sensor data in the tap-hammer setup, achieving a correlation of 0.98 and a root mean square error (RMSE) of 1.437 inches (39.5 mm). For the drop-weight setup, the best outcomes were from a user-defined GB model trained on Acl sensors, with similar correlation and a lower RMSE of 1.176 inches (29.87 mm). For energy prediction, models were less effective compared to position prediction. The user-defined GB model on Mis sensor data provided the best tap-hammer results, with a correlation of 0.90 and a RMSE of 5.847 mV·ms. For the drop-weight setup, the optimized GB model on Acl sensor data yielded the best results, with a similar correlation but a higher RMSE of 8.664 mV·ms.

This experiment highlighted the potential of using machine learning models to detect, locate, and characterize impact events in a complex aircraft structure. This capability is crucial for enhancing aircraft maintenance by facilitating automated early detection and evaluation of impact damage; thereby, providing essential information to maintain structural integrity.

6.1.3 **REFERENCES**

[13] Pant, S., Wooldrige, J., Seabrook, E., Valdes, J., Genest, M., SHM to detect and characterize impact events in metallic aircraft structure, 11th European Workshop on Structural Health Monitoring, 10 – 13 June 2024, Potsdam, Germany.

6.2 Digital Detector Array (DDA) for Non-Destructive Radiographic Image of Aircraft Structural Components

Muzibur Khan, NRC Aerospace

For the safety and airworthiness of aircraft, the aerospace industry has stringent product quality requirements to ensure structural integrity of critical components. Non-destructive inspections (NDI) are routinely performed to ensure product quality and identify defects before they reach critical sizes. Radiographic inspection plays a key role for inspection of aircraft structural components. Film-based radiography requires consumables, a darkroom facility, and manual processing; this is not only time consuming, but also requires more radiation exposure than digital systems. Digital radiography, which eliminates these requirements, is currently in a transition state of switching to two kinds of digital technologies: (1) Digital radiography (DR), using flat panel detectors, commonly known as Digital Detector Arrays (DDA)., and (2) Computed Radiography (CR). Flat panel detector (DDA) based technology allows faster/easier straight acquisition of the radiographic image digitally without using films or even phosphorous plate like in CR. DR/DDA is also suitable for real time imaging and automation. Before implementing this technology in aircraft inspection, a detailed performance assessment is required to qualify it.

Digital Detector Arrays (DDA) based digital radiography system convert X-rays or gamma rays into light, which is then converted into an electric signal (voltage) and is subsequently sampled to form the digital image. DDA or DR allows faster/easier acquisition of the radiographic image digitally without using films, chemicals or phosphorous plate. DR/DDA is also suitable for real time imaging which makes it suitable for automating some processes. As claimed by the DDA manufacturers the typical advantages are, highest throughput; imaging results immediately available for review (without intermittent process like scanning); ability to optimize exposure setting live during the inspection; higher SNR; no moving parts or wear items; ability to use digital image processing like filter; zoom measurement; and no scratch artifact in the image. The speeds of these devices can range from many seconds per image to many images per second, up to and exceeding real-time radioscopy rates (usually 30 frames per second).

Despite the numerous benefits when compared to conventional film, the widespread application of DR/DDA still poses significant challenges for end users such as, a steep learning curve/know-how of the processes, lack of procedures to choose parameters, lack of demonstrated system performance, image quality indicators, image lag, bad pixel correction etc.

The National Research Council of Canada has been tasked by the Royal Canadian Air Force (RCAF) for developing documentation for the performance evaluation of the flat panel Digital Radiography DR (digital detector array or DDA) technology. In this assessment campaign, the ASTM E2737 “Standard Practice for Digital Detector Array Performance Evaluation and Long-

Term Stability" is used to measure the baseline performance of the of the DDA. A set of performance attributes/parameters is defined to evaluate the performance of a digital detector array imaging system. The core image quality parameters are spatial resolution (i.e., effective pixel size), contrast sensitivity, SNR, the signal level, bad pixel distribution and contrast-to-noise ratio (CNR). The inspection part specific parameter is the evaluation of material thickness range. The ASTM E2737 recommends that quality evaluation tools (phantom) are used to measure some of the key parameters of the DDA imaging system.

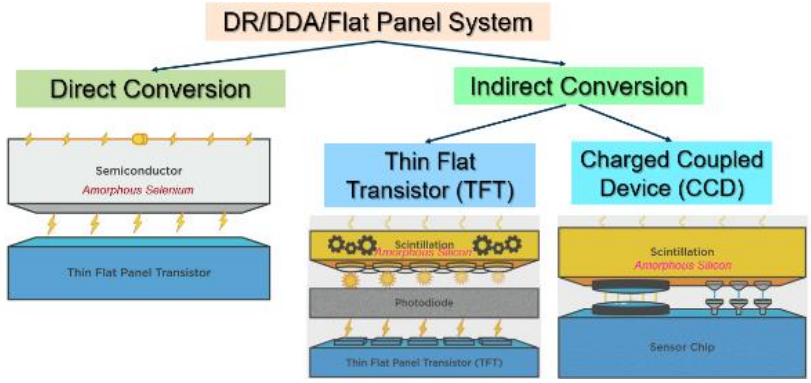

Figure 19: DDA Flat Panel Radiography System.

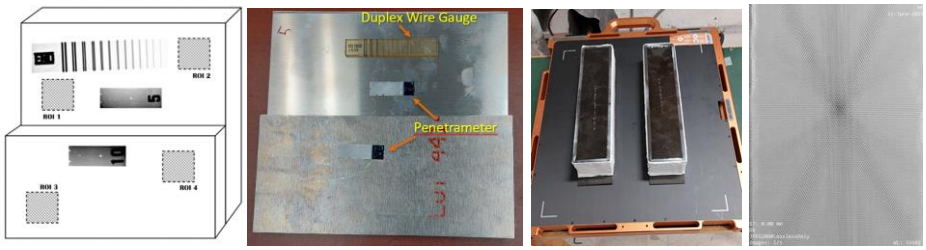

Figure 20: Duplex Plate Phantom setup and a sample composite specimen.

6.2.1 REFERENCES

[14] Khan. M, "Digital Detector Array for Non-destructive Radiographic Imaging of Aircraft Structures" Journal of Canadian Institute for Non-destructive Evaluation (CINDE), Vol. 45, No. 3, September 2024.

7.0 FATIGUE AND STRUCTURAL INTEGRITY OF COMPOSITES

7.1 Damage Modelling of an F/A-18 Ti-to-Composite Lap Joint for Assessing Residual Strength

Gang Li, NRC Aerospace

In collaboration with the Royal Canadian Air Force, armasuisse, the United States Navy, RUAG, and L3 Harris, NRC conducted a full-scale fatigue test to gain a better understanding of the effect of a partially disbonded Inner Wing Step Lap Joint (IWSLJ) on the structural integrity of the F/A-18 wing (see Section 2.1). In a separate project funded by DRDC-DND, NRC developed numerical modelling, including global and local finite element models (see Figure 21) to determine the effect of the disbond on the joint residual strength (RS).

7.1.1 TEST DATA

The F/A-18 IWSLJ test underwent three phases: (i) a strain survey of three load cases, (ii) cyclic fatigue loading under a representative load case, and (iii) residual strength testing for two load cases. The tests were performed at room temperature, with loads scaled up to account for temperature effects. In addition to monitoring the displacements at the actuator loading points, strain gauges, data image correlation (DIC), and fibre optic strain sensors were employed to collect strain and displacement data. At given intervals, NDI inspections, including manual ultrasonic technique (UT), automated UT (TecScan Armanda, by QETE), and general and detail visual observation, were conducted to monitor disbond growth.

7.1.2 VALIDATION OF GLOBAL AND LOCAL SUB-MODELLING

Global Nastran FE analyses were conducted under representative load cases. A local region within Bay 3 was modelled using the virtual crack closure technique (VCCT) and displacement boundary conditions extracted from global finite element analyses (GFEA). Wing spanwise strains showed good agreement between the test and the numerical results, as illustrated in Figure 22 and Figure 23.

7.1.3 RESIDUAL STRENGTH ASSESSMENT AND CONCLUDING REMARKS

The validated local FE analysis (LFEA) approach was utilized to assess the joint residual strength using the mixed-mode BK damage evolution criterion. The onset of disbond damage growth was determined, and the residual strength was evaluated under two possible fracture failure conditions. The predicted residual strengths were approximately: (i) 1.5 times the design limit load (DLL) using composite laminate delamination properties, and (ii) 3.1DLL for cohesive damage fracture within the FM-300K adhesive layer, dominated by adhesive fracture toughness properties. The

assessment assumed a full-width, symmetric disbond profile at the top and bottom step faces. In the full-scale residual strength test, a load case of 1.37DLL was applied without failure.

Future applications of the LFEA will study the influence of other representative disbond scenarios and load cases on the residual strength. Also, DIC data will be utilized for measuring experimental disbond growth and supporting the development of numerical models to replicate and predict more complex disbond scenarios.

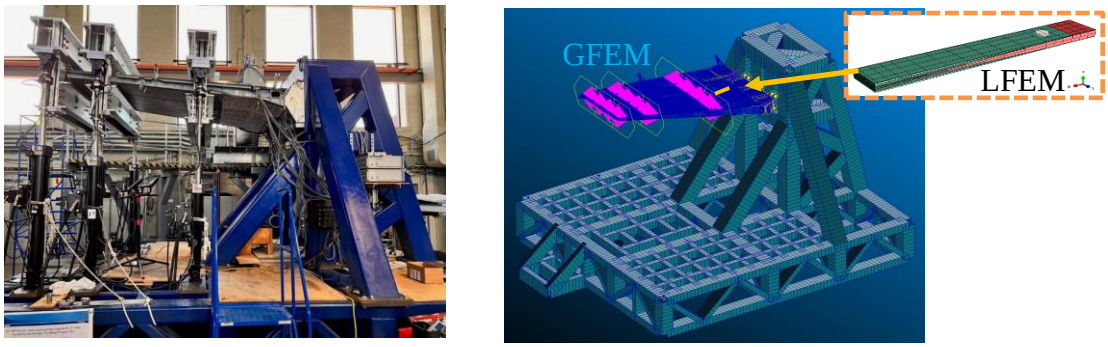

Figure 21: Test article setup, global and local FE models.

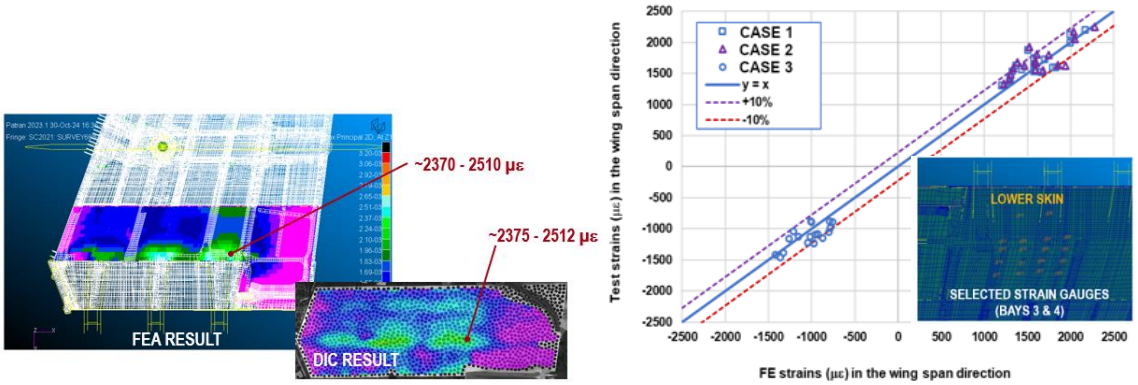

Figure 22: Strain comparisons between measurements and GFEA results on the lower skin.

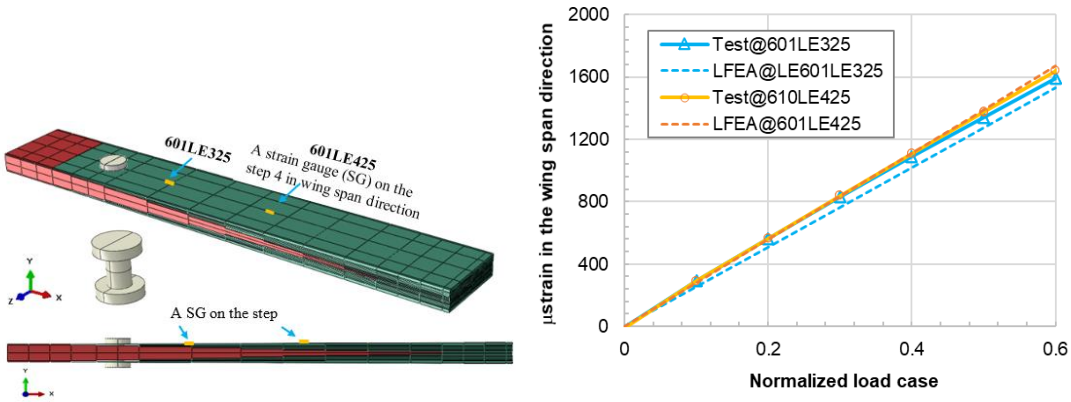

Figure 23: Local FE analysis (LFEA) validation through strain comparisons.

7.1.4 REFERENCES

Li, G., Renaud, G., Dionne, E, Brunet S., Bombardier, Y., CF-188 Hybrid Inner-Wing Step-Lap Joint Damage Modelling (NRC, CP-SMM-2025-0029), Presentation of the 2025 Holistic Structural Integrity Process (HOLSIP), 24-28 February 2025, Virginia, USA.

7.2 Development of Numerical Modelling for Assessing Disbond and Strength of a F/A-18 Step-Lap Joint Specimen

Gang Li, NRC Aerospace

In this study, the virtual crack closure technique (VCCT) and cohesive zone modelling (CZM) were employed to simulate disbond failure behaviour for assessing residual strength of an assumed 25.4 mm wide F/A-18 inner wing step-lap joint (IWSLJ) specimen, following the identification of an appropriate mesh condition.

7.2.1 MODELLING DISBOND FAILURE BEHAVIOUR AND RESIDUAL STRENGTH

In addition to the VCCT and CZM techniques, the ultimate strain of the FM300K adhesive material was used to assess joint strength under three joint bonding conditions. Minimal differences in predicted strength were observed from the cohesive zone elements using different cohesive strengths values. The FE models and three bonding conditions are shown in Figure 24. Strength comparisons between test and numerical results are presented in Table 3. Very good agreement in joint strength was obtained between a DSTG test result and the current VCCT analysis results using the delamination fracture properties of IM7/977-3 tapes.

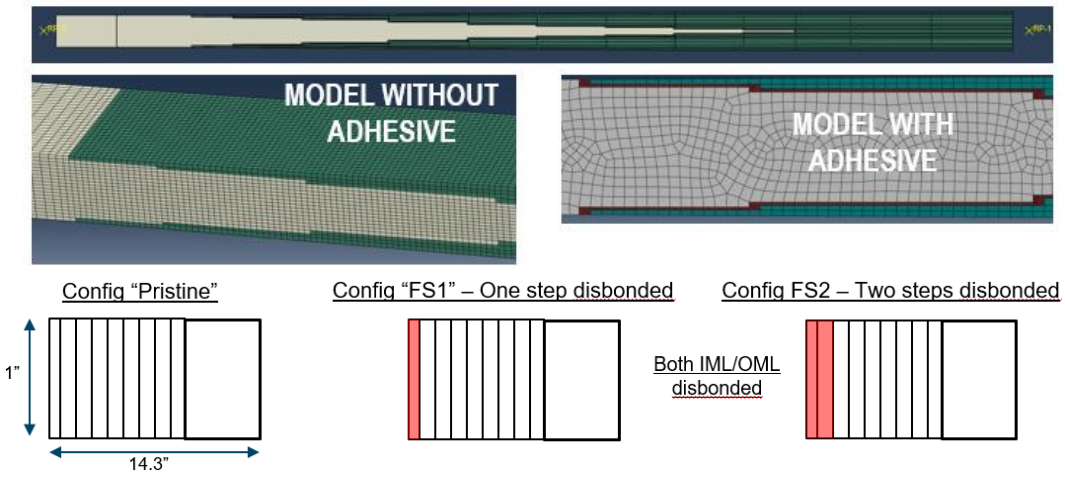

Figure 24: Finite element models for the F/A-18 IWSLJ specimen in three bond conditions.

Table 3: Failure loads of the bonded F/A-18 IWSLJ specimen

Bond condition	DSTG (converted results)	NRC FE analyses			
	Test	Adhesive-centre (adhesive strain)	VCCT (adhesive fracture)	VCCT (IM7 fracture)	CZM (IM7 fracture
Pristine	---	271 kN	345 kN	161 kN	184 kN
FS1	---	205 kN	265 kN	125 kN	121 kN
FS2	**93.1 kN**	135 kN	190 kN	**93 kN**	79 kN

7.3 Effective Hybrid Damage Modeling Framework for Composite Laminate Strength Predictions

Gang Qi, Heng (Hannah) Liu, NRC Aerospace, Il Yong Kim, Queen's University, Diane Wowk, Royal Military College of Canada (RMC)

7.3.1 HYBRID DAMAGE MODELING FRAMEWORK

A reliable hybrid modeling and simulation methodology is being developed at NRC Aerospace to predict the progressive damage evolution and ultimate strength of multidirectional fiber-reinforced polymer (FRP) composite laminates. The modeling approach integrates continuum damage modeling (CDM) and discrete damage modeling (DDM), to capture fiber breakage, matrix major cracking, composite ply interlaminar delamination, and the interactions of these failure modes. In particular, four main components form the hybrid modeling framework, as presented in Fig. 1. The Schapery theory is incorporated into the finite element (FE) model to accurately simulate the pre-

peak nonlinearity of the load-bearing response caused by matrix micro-cracking. While the extended finite element method (XFEM) is used to capture matrix major crack propagation, continuum damage modeling (CDM) via the modified 3-D Hashin's failure criteria with a zigzag stiffness degradation is used to capture fiber failures. The cohesive zone modeling (CZM) technique is used to model interlaminar failure (composite delamination). Such a computational mechanics framework is implemented in Fortran-coded "UMAT" and "UDMGINI" user subroutines, integrated with the Abaqus/Standard solver.

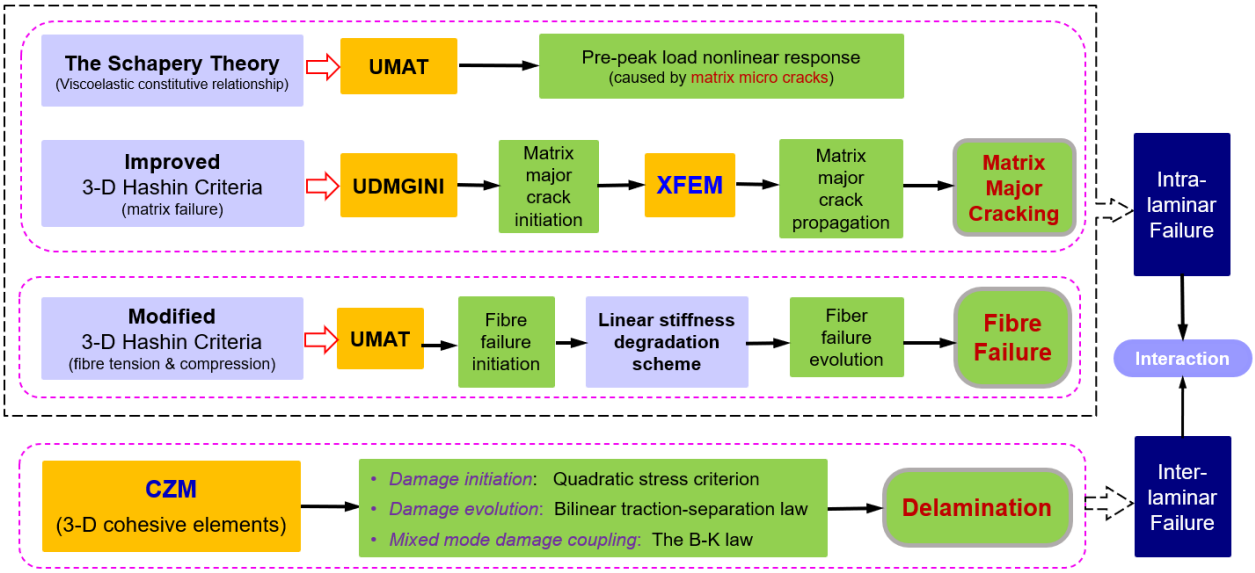

Figure 25: Composite laminate hybrid damage modeling framework.

7.3.2 FE MODELING CASE STUDIES

Four typical composite panel configurations, open-hole tension (OHT), open-hole compression (OHC), filled-hole tension (FHT), and filled-hole compression (FHC), were examined as case studies. As illustrated in Fig. 2, each FE model had the quasi-isotropic lay-up [45/90/-45/0]s with a total panel thickness of 1.162 mm, and the center diameter of the hole size was 3.175 mm. Each composite ply was modeled using a single layer of 3-D 8-node solid elements, and each interface between two adjacent composite plies with different angles was embedded using a single layer of zero-thickness 3-D cohesive elements. The material properties of T800/3900-2 unidirectional prepreg was used in this study.

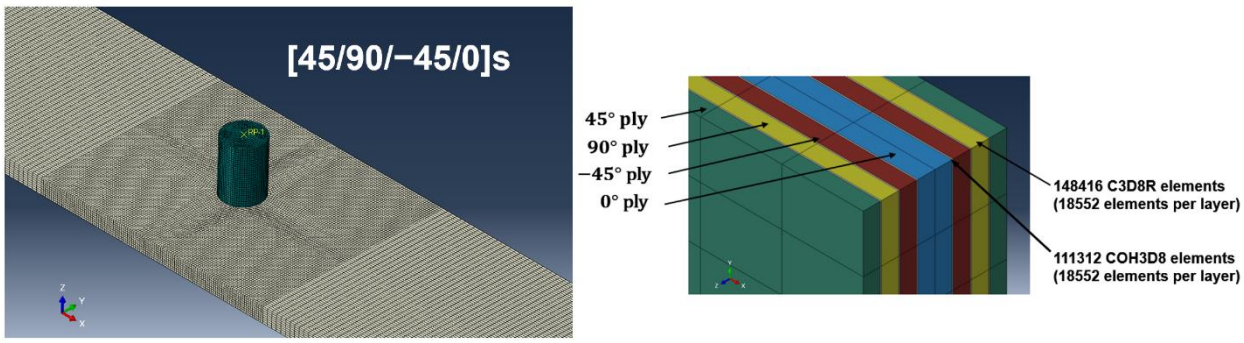

Figure 26: Filled-hole tension FE model.

7.3.3 MODEL RESULTS AND CONCLUSIONS

It was shown that the models can predict matrix crack paths for all plies and delamination patterns in all the considered panel configurations. Local stress redistribution, which is very important for accurately predicting a panel's ultimate strength, is adequately exhibited in the simulations. Furthermore, the models can capture the fiber stress relation on 0˚ plies due to longitudinal splitting, which is very important for accurately predicting the ultimate strength and delamination migration. Results also indicated that matrix cracks can promote local delamination. Overall, a good correlation was obtained between the simulations and experiments from open literature.

Without sophisticated meshing schemes and extensive contact definitions, this hybrid modeling framework and methodology is shown to be an effective and efficient tool to model the complex composite damage progression and properly predict the ultimate strengths of the laminates.

7.3.4 REFERENCES

[15] Qi, G., Liu, H., Kim, I.Y., Wowk, D., The application of a hybrid damage modeling and simulation methodology to composite laminate residual strength predictions, Proceedings of the 8th International Conference on Frontiers of Composite Materials (ICFCM 2025), June 9-11, 2025, Tokyo, Japan.

7.4 Experimental Study and Numerical Prediction of Buckling of Composite Panels

Lucy Li, NRC Aerospace

Aircraft structures such as wings are subjected to compressive loading. Buckling, characterized by a sudden out-of-plane deflection of a structural member under compressive loading, can lead to structure failure. The National Research Council of Canada has investigated low-velocity impact (LVI) resistance and post-damage load carrying capabilities through compression after impact

(CAI) tests of composite laminates, highlighting the physics of global buckling and its effect on the structural strength.

7.4.1 EXPERIMENTAL STUDY

In this work, composite compression testing was conducted following modified ASTM D7136 and ASTM D7137 standards, for larger test panels of 254 mm × 305 mm × 4.3 mm [10” × 12” × 0.171”]. Unstiffen panels were fabricated with IM7/977-3 carbon fiber prepreg and a layup sequence of $[0/45/90/-45]_{4s}$. A hemispherical impactor tip of 25.4mm [1”] in diameter and a mass of 6.25 kg was positioned at a calculated height based on the desired impact energy (30 J or 75 J). An ultrasonic C-scan using Tecscan immersion system was performed on the impacted panels at 5 MHz with 12.7 mm [0.5”] flat immersion probe. Following the impact, the uniaxial compression test was conducted according to a modified ASTM D7137. Figure 27 shows the two test configurations: a) ASTM-equivalent support fixture (NS) that allows for global buckling, and b) Fixture with *additional* front/back support plates (S) to supress the global buckling. This test method allows for two options of expected compressive behaviour of test panels, either driven primarily by global buckling or by localized damages. A combination of four different scenarios for the impact testing and two scenarios for the CAI tests was used for a total of eight different evaluated test conditions as shown in Figure 27c.

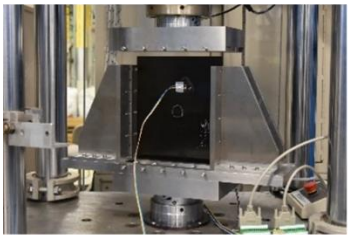

a) ASTM-equivalent support fixture

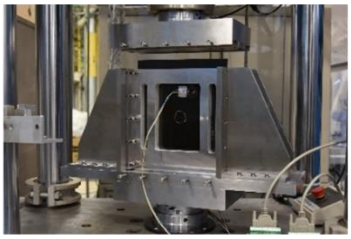

b) Fixture with additional support plates

Impact conditions	Number of panels	Compression testing conditions
Pristine (No impact)	1	Unsupported (NS): with an unsupported area of 248 mm by 269 mm
30 J	2	
75 J	2	
30 J x3 (multi-hit)	1	
Pristine (No impact)	1	Supported (S): with an unsupported area of 127 mm by 178 mm
30 J	2	
75 J	2	
30 J x3 (multi-hit)	2	

c) Impact and CAI testing conditions

Figure 27. Compression test with a) ASTM-equivalent support fixture and b) fixture with *additional* front/back support plates, c) Test conditions for impact and compression after impact testing.

The resultant impact damage, as shown in Figure 28, ranged from no visible damage to significant visible damage. Figure 28b shows the post-impact surface damage difference between the two impact energy levels of 30 J and 75 J, and it also shows the internal damage caused by the impact. Panels hit with 30 J of energy had barely visible damage on the front and back surface, and the panels hit with 75 J had a clear dent at the front with fiber breakage at the back. NDI C-scans on the panels tested at 30 J had an average maximum internal damage diameter of 35 mm ± 2 mm, while the panels tested at 75 J had an average damage diameter of 53 mm ± 5 mm.

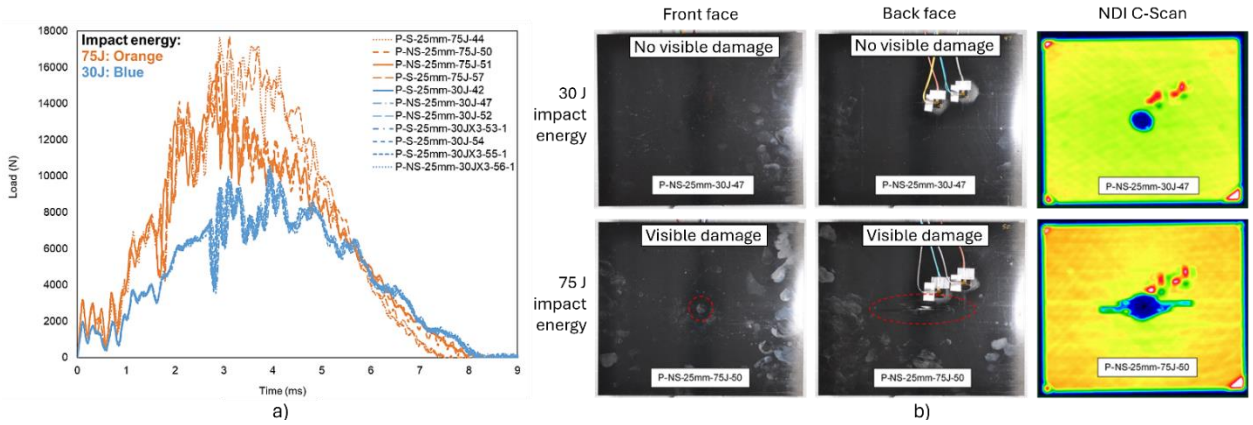

Figure 28. a) Load over time response of panels subject to impact energy of 30J or 75J, b) Post impact images of panels subject to 30J or 75J.

CAI tests were conducted with or without additional anti-buckling plates as shown in Figure 3. The pristine (w/o additional support) specimens and those impacted at 30 J or 75 J energy levels had an average strength of 193 MPa with no clear distinction in their ultimate strengths. In comparison, the panels with additional support plates showed a linear response of stress vs. strain, with an increased ultimate residual strength. There is also a distinction between the results of the different test conditions, where the panels impacted with the higher energy level of 75 J reached failure at around 220 MPa, the panels impacted with 30 J reached failure at around 250 MPa and the pristine panels had the highest compressive strength and reached failure at around 300 MPa.

Post-CAI pictures of the panels are shown in Figure 29, which shows the difference in damage propagation between the supported and unsupported panels. Panels that were unsupported had damage propagating from the edges of the panels and off-centered with the impact damage site, whereas the panels that were supported had damage propagating from the impact damage site along the transversal axis of the panel. These results were consistent for all the test samples.

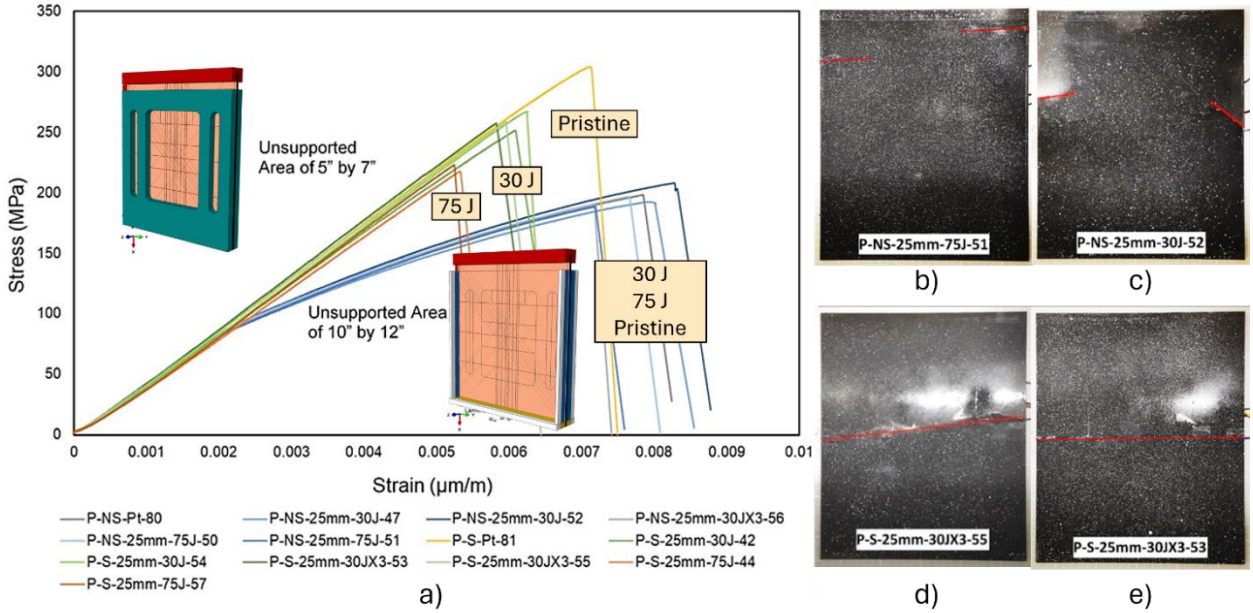

Figure 29. a) Compression after impact response of supported and unsupported panels with two impact energy levels. Damage propagation mechanisms of b), c) unsupported; and d), e) supported panels.

7.4.2 HIGH-FIDELITY MODELING OF COMPOSITE BUCKLING

NCProCDM, a high-fidelity code for ABAQUS, jointly developed by NRC and Carleton University, was applied to this study. This physics-based finite element (FE) prediction tool provides damage evolution and damage characteristics such as delamination, matrix cracking, fibre kinking, splitting and tensile failure as well as their interactions. Figure 30 shows the prediction results of the cases with and without additional anti-buckling plate, showing the capability of the code to capture onset of buckling, as well as the ultimate strength. The simulations also showed the different failure modes, where failure of the composite panels with additional support plates was initiated from local buckling in the form of fibre kinking and splitting near the dent, and the panels without additional support plates exhibited global buckling and failure initiated from the edge of the panels first upon contact.

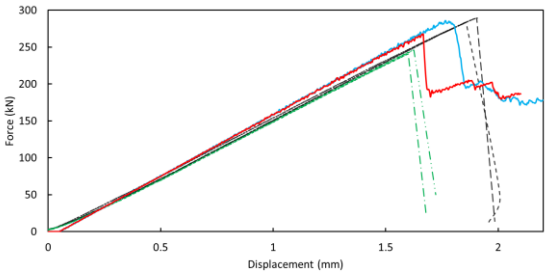

With support plates - 30J impact	
	CAI strength (kN)
Experiment (42)	283.2
Experiment (54)	289.2
Average	**286.2**
Model (2)	**285.8**
Difference	**-0.1%**

With support plates - 75J impact	
	CAI strength (kN)
Experiment (44)	245.8
Experiment (57)	240.8
Average	**243.3**
Model (3)	**267.6**
Difference	**+9.0%**

(a) with additional support

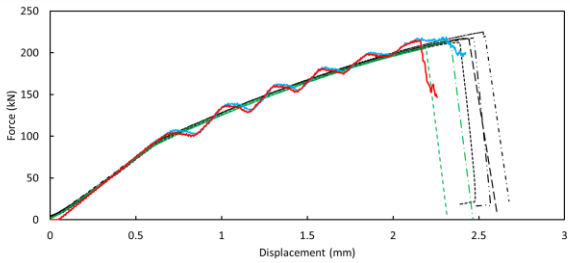

Without support plates - 30J impact	
	CAI strength (kN)
Experiment (34)	217.6
Experiment (36)	212.1
Experiment (47)	217.7
Experiment (52)	224.8
Average	**218.0**
Model (39)	**218.7**
Difference	**+0.3%**

Without support plates - 75J impact	
	CAI strength (kN)
Experiment (50)	213.4
Experiment (51)	205.3
Average	**209.4**
Model (1)	**214.7**
Difference	**+2.5%**

37

(b) without additional support

Figure 4 Experimental results and high-fidelity FEA prediction of compression after impact of the tested panel.

7.4.3 SUMMARY

This composite buckling study exhibited distinctly different responses of composite panels subject to compression after impact, where a linear response and higher residual compression strength were observed for the test panels with reduced unsupported area, and a non-linear behaviour and lower compression strength for the larger unsupported area prior to failure. This study illustrated the role of global buckling in reducing load-carrying capabilities of composite panels subjected to impact damage at 30J and 75J by as high as 144% and 178%, respectively. This study also illustrated how global buckling is affected by damage onset and propagation mechanisms of composite laminates in compression.

The NCProCDM code not only predicted well the buckling of composites, it also provided physics-based explanation of the reasons behind the failure mechanisms. The failure of the composite panels with support plates initiated near the dent due to local buckling in the form of fibre kinking and splitting, followed by sudden failure. In comparison, the panels without additional support plates exhibited global buckling, which was well captured in simulation. As a result, and the ultimate strength is irrelevant of the damage sizes in this case.

7.4.4 REFERENCES

[16] Li, L., Vallee, J., Shabani, P., Laliberte, J., And Dondish, A., Understanding the Effect of Global Buckling on Composites Damage Tolerance, Proceedings of Canadian International Conference on Composite Materials, (Cancom2024), Waterloo, Canada, Aug 2024.

7.5 Strength Design Assessment of a Wind Tunnel Composite Rotor Blade

Gang Li and Jihua Chen, NRC Aerospace

The National Research Council of Canada initiated an internal project to develop composite rotor blades as replacements for the existing blades made from G10 glass material to enhance the performance of an NRC wind tunnel [17]. The current G10 material blades frequently encounter issues such as damage from ice pellet impacts, water infiltration, delamination, and debonding. In this effort, composite blades were developed using carbon and glass fibre-reinforced thermoplastic composites. These thermoplastic composites boast superior mechanical properties with high specific stiffness and strength. Additionally, they offer other benefits, such as corrosion resistance, fatigue resistance, vibration damping, recyclability, and repairability.

7.5.1 BLADE DEFORMATIONS AND PEAK STRESSES UNDER TWO LOAD CASES

A combination of multiple 8-ply unit laminates with an "optimal" layup was used to design the composite blade structure for superior performance. The optimal layup for the 8-ply unit laminate was determined through theoretical analyses of effective stiffness parameters across six symmetric layups, ensuring adequate stiffness in bending, torsion, tension, and shear.

Using the identified layup sequence, a three-dimensional finite element model was developed (see Figure 30). Simulations of the designed composite blades were conducted under bending and longitudinal tensile loadings. The blade stiffness and the associated peak stresses were investigated for four different CFRP composite materials, in addition to the G10 glass material.

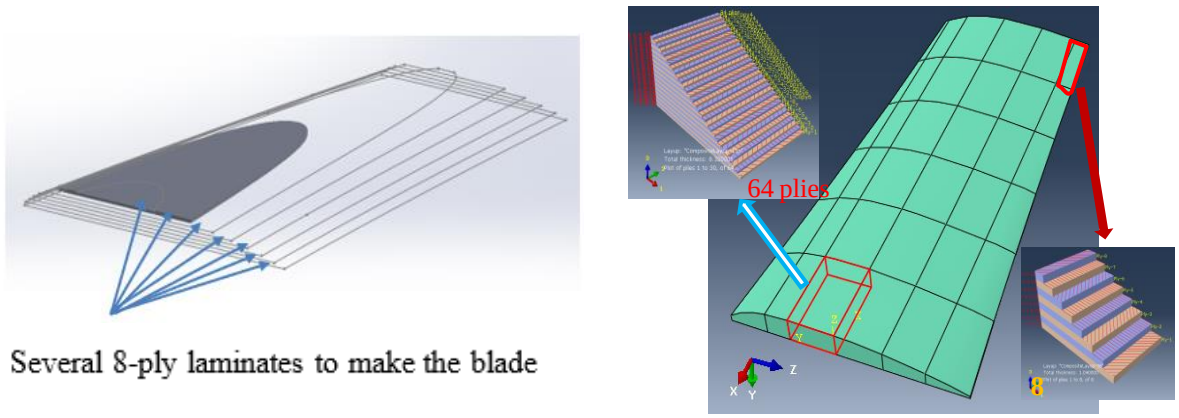

Figure 30: Schematic diagram to show a composite blade and its FE model made using multiple 8-ply laminates.

7.5.2 RESULTS AND CONCLUDING REMARKS

The resulting load-displacement curves are presented in Figure 31. Good agreement was obtained between test and numerical results for the G10 material blade under both bending and tensile loading scenarios. A significant improvement in stiffness was achieved by using the CFRP materials compared to the G10 material. Also, a strength safety factor of 3 was obtained for the CFRP blade.

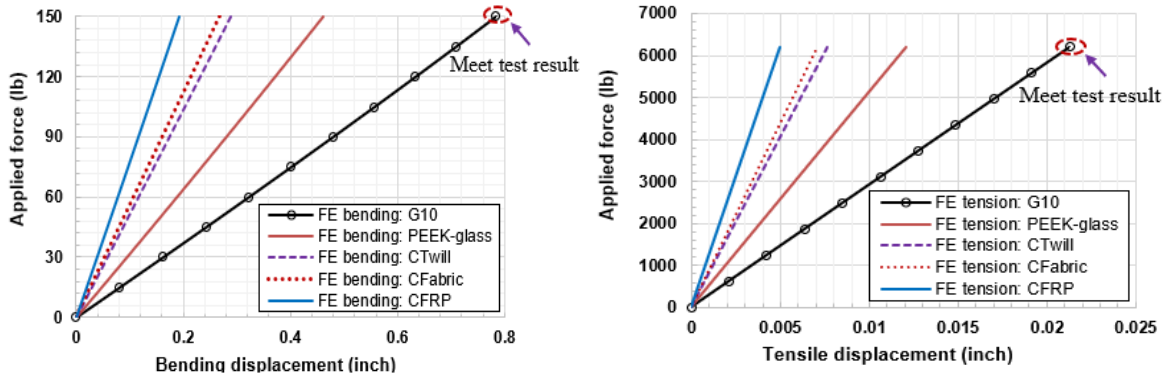

Figure 31: Comparison of the load-displacement curves of the composite blade under bending and tension.

7.5.3 REFERENCES

[17] Li, G., Chen, J.H., Perrier, P., St Stiffness and Strength Design Assessments of a Composite Rotor Blade for the NRC's Altitude Icing Wind Tunnel Located at Aerodynamics Laboratory, Lab Technical Report, LTR-SMM-2023-0170, September 2023, NRC Aerospace, Ottawa, Canada.

8.0 FATIGUE AND STRUCTURAL INTEGRITY OF NEW MATERIALS AND MANUFACTURING

8.1 Advancements in Certifying Additively Manufactured Primary Structural Components for Aerospace Use

David Backman, Priti Wanjara, Sheida Sarafan, NRC Aerospace

One of the essential factors for incorporating additively manufactured structural parts into mainstream aviation is the capability to certify these parts as airworthy. This project update outlines the pivotal results of the certification-like testing approach employed for additively manufactured Ti-6Al-4V corner fittings (brackets), produced using electron beam welding (EBW) technology for the CP-140 Aurora aircraft.

Previous testing, as reported in the ICAF 2023 Canadian National Review, examined several iterations of the brackets, subjecting them to both static and fatigue loads necessary for potential certification. The static test involved applying design limit and ultimate loads, while the fatigue test required the brackets to endure two lifetimes of spectrum fatigue loading. Until recently, the performance of the brackets could not be benchmarked against the OEM 7075 aluminum bracket (Figure 32(a)). Testing an OEM bracket has opened the possibility for topology optimization to reduce the inherent stiffness gain due to the higher modulus of Ti-6Al-4V, aiming to produce a bracket with stiffness comparable to the OEM bracket while still meeting all static and fatigue certification requirements. This update provides an overview of the results from a bracket manufactured using the electron beam melting process (Ti-6Al-4V, Figure 32(b)), compares the results to the OEM bracket (aluminum 7075), and evaluates the performance against a topology-optimized bracket produced using laser powder bed manufacturing (Ti-6Al-4V, Figure 32(c)).

The primary objective of topology optimization for the titanium bracket was to achieve mechanical properties, particularly stiffness, that are comparable to those of the OEM aluminum bracket while leveraging the superior material characteristics of Ti-6Al-4V. This involves redesigning the bracket's geometry to effectively manage strain distribution, thereby minimizing the inherent stiffness gain due to the higher elastic modulus of titanium compared to aluminum. The current iteration of the optimized bracket was produced by Australia's Defence Science and Technology Group (DSTG) using a generative optimization process. This approach intends to maximize the potential of additive manufacturing technologies in addressing the common requirement to replace aerospace-grade, non-weldable aluminum alloys such as 7075 with titanium, while reducing the risk associated with strain mismatch between the titanium part and surrounding structures.

The test results showed that the electron beam melting process successfully produced high-quality, certifiable parts in both the as-machined and HIP’d conditions. During the static certification

loading, a maximum ultimate limit load of approximately 118 kN (26,500 lbf) was applied to each bracket. The overall strain results, monitored by a 3D digital image correlation (DIC) system, are illustrated in Figure 33, showing a strain concentration in the transition region between the base of the bracket and its tapered side wall. Additional DIC images (Figure 34) were taken post-test to assess whether any residual (plastic) strains had been induced in the samples. Figure 34 clearly shows that the OEM bracket exhibited a small region of plastic residual strain in this transition zone.

Due to limitations in individual specimens from each additive manufacturing (AM) process, static and fatigue testing were combined. Consequently, all brackets transitioned from static testing to the fatigue testing phase of the certification approach. Table 4 provides a concise summary of the fatigue testing results following to the static testing. Overall, the bracket manufactured using the Electron Beam Welding (EBW) process exhibited the longest fatigue life, with the steel fixture retention bolt failing before any visible cracking occurred. The topology-optimized bracket (LPBW) had the next longest fatigue life, with failure occurring in the body of the bracket shortly after the start of the fourth lifecycle (LC) of testing. The fatigue life of the OEM bracket was the shortest, failing just before the end of the second LC. Although the OEM bracket did not pass the testing outlined in this demonstration certification program, it should be noted that if more test brackets had been available, static and fatigue testing should have been conducted on separate pristine specimens.

This project highlights the significant progress made in certifying additively manufactured components for aerospace applications, underscoring the potential for further optimization and integration into primary structural application.

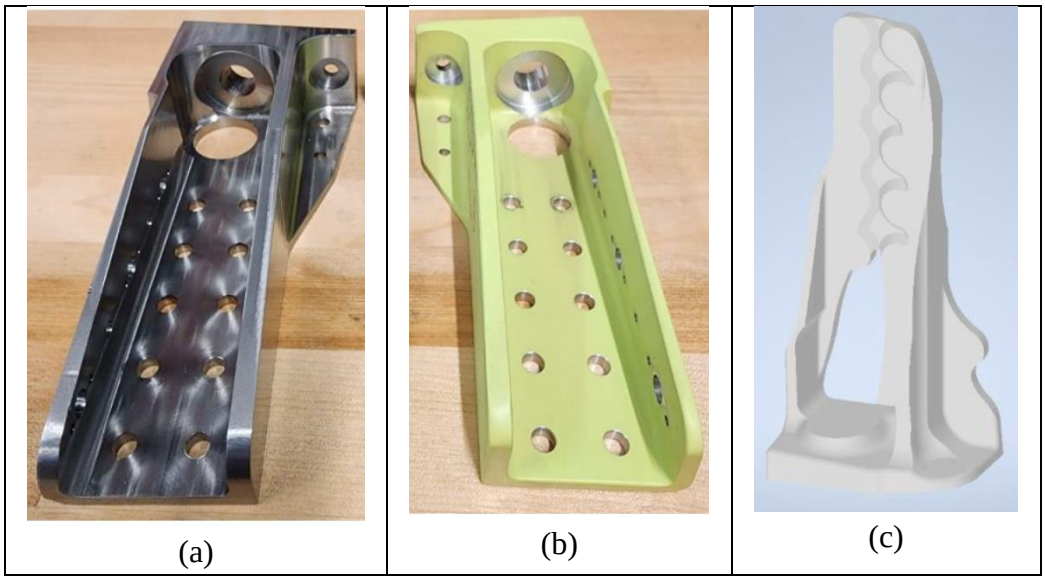

Figure 32: (a) EBW bracket (b) OEM bracket (c) CAD model of LPBW optimized bracket.

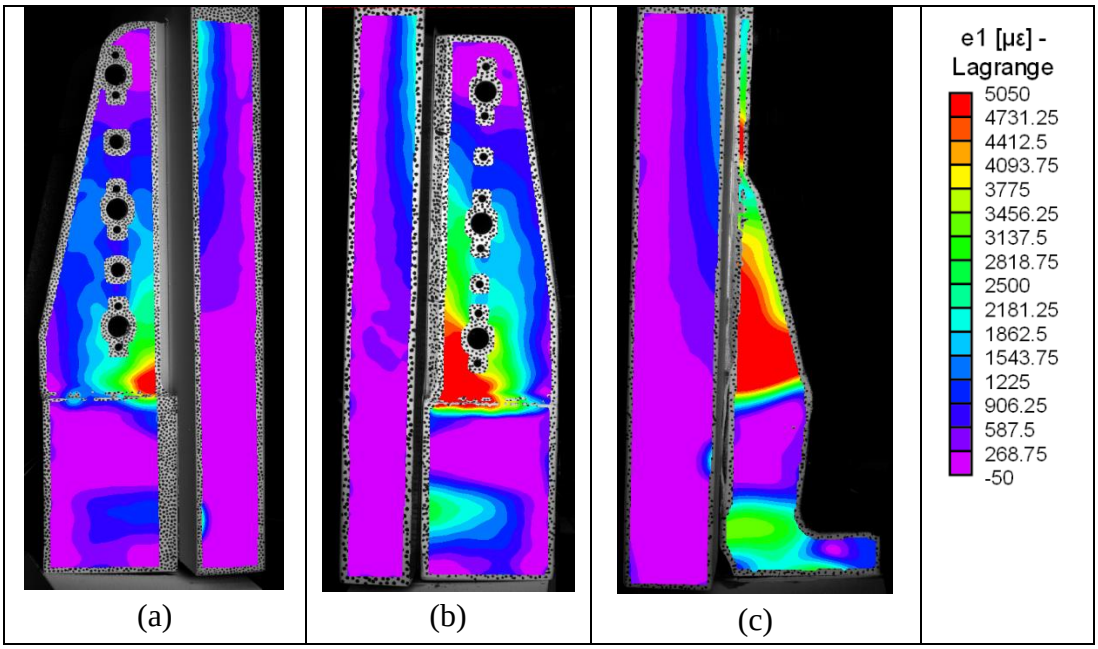

Figure 33: Static ultimate load strains: (a) EBW bracket (b) OEM bracket (c) LPBW bracket – optimized.

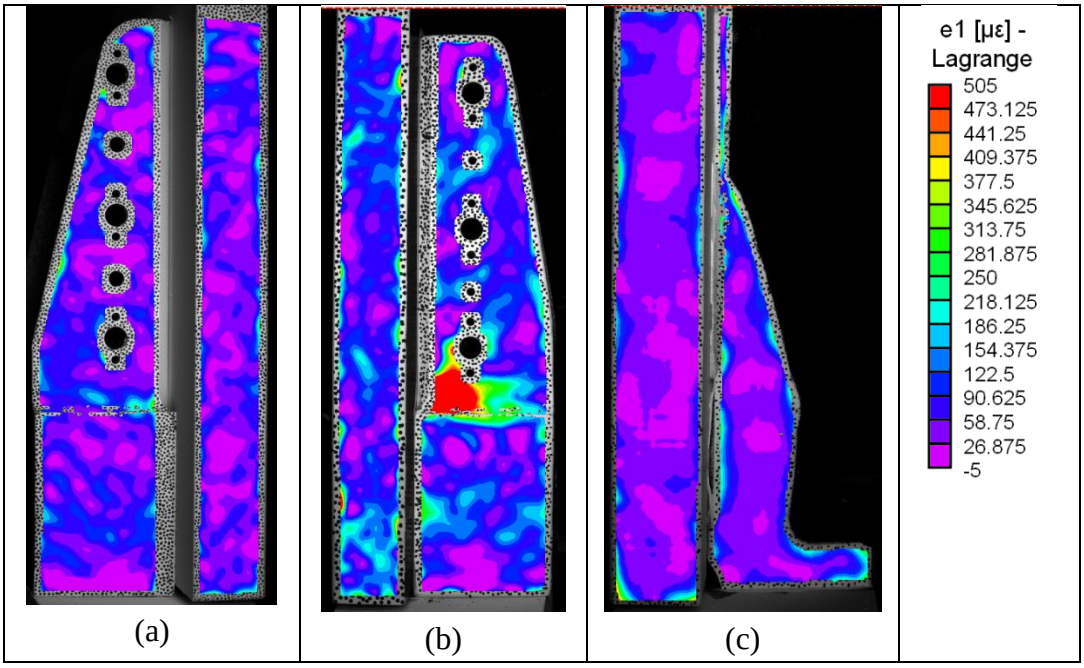

Figure 34: Post static loading strains: (a) EBW bracket (b) OEM bracket (c) LPBW bracket – optimized.

Table 4: Summary of bracket certification like testing

	Bracket 5 (Sckiacky)	**Bracket 6 (OEM)**	**Bracket 7 (Optimized)**
Static Load	Passed	Passed [residual strain noted]	Passed
Fatigue Spectrum (2 Full Lifecycles)	Passed	Failed	Passed
Final Failure	n/a [LC4]	LC2, Block 7	LC4, Block 1
Failure Mode	Retention bolt failed	Body of bracket	Body of bracket

8.2 Fatigue Failure of Thermal Barrier Coatings under Thermal Cycling Environments: Multi-physics Modeling

Kuiying Chen, NRC Aerospace

Under the support of DRDC, DTAES and in collaboration with NATO, the National Research Council of Canada (NRC) has been carrying out thermal fatigue failure analysis of air plasma spray thermal barrier coatings (APS-TBCs), Figure 35, under adverse environments of 1050 ^{o}C /1-hour for 30 cycles using COMSOL multi-physics modelling methodologies. The delamination failure of TBCs typically occurs at interfaces between the topcoat and bond coat due to thermal mismatch stress and thermal gradient, resulting in fatigue crack propagation and coating final spallation failure. Heat transfer was cyclically implemented into the TBC model, resulting in a thermal gradient, aimed at simulating the in-service operation of the TBC system. A variational-based sintering model for a topcoat of TBCs is incorporated into the simulation. The high-temperature creep model of the topcoat, thermal growth oxide (TGO) and bond coat are included. Combining the TGO growth during thermal exposure, the TGO growth accelerates the moving of the maximum stress toward the valley location of the interface. The steeper roughness of the interface accumulates stress due to the greater thermal mismatch strain. The sintering of the topcoat strongly affects stress at the later stages of the coating life.

Phase field damage [18] modelling indicates that the crack at the off-peak interface propagates rapidly towards the top right direction in the first few cycles, as shown in Figure 36, then stops propagating as the TGO thickens because the location of maximum principal stress is moved away. Due to the accumulated stress at the crack tip at the end of cycles, cracks have the potential to propagate with a prolonged thermal cycle service, Figure 37**.**

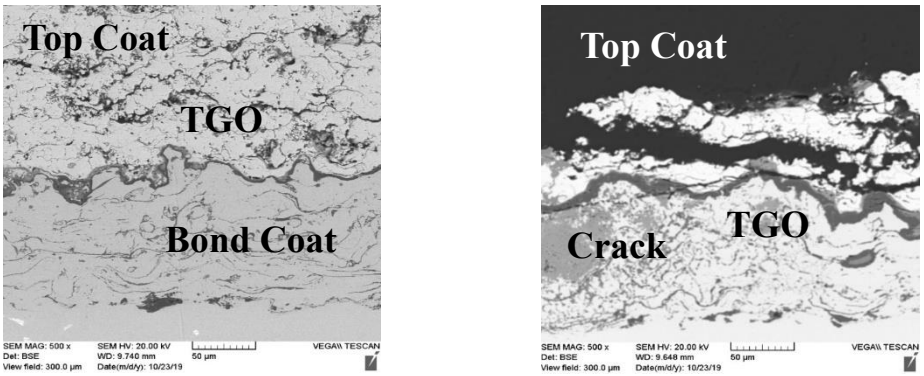

Figure 35: Air plasma spray thermal barrier coatings (APS-TBCs) for gas turbine engines.

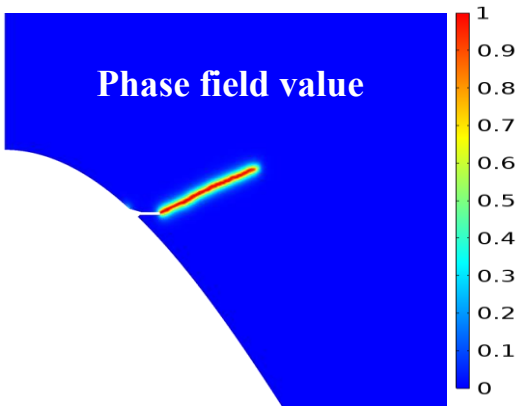

Figure 36: Phase field evolution at cycle # 7 upon TGO growth.

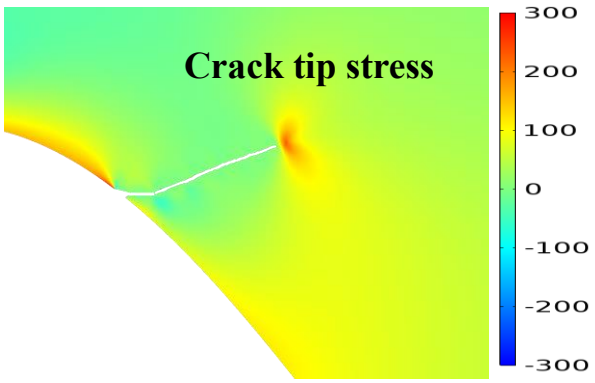

Figure 37: Principal stress concentration evolution upon TGO growth at cycle #7. The crack tip stress decreases as the stress concentration center moves away.

In summary, the TGO thickness is the primary factor to affect stress concentration, with a higher aspect ratio of an interface, the stress concentration center is less affected by the TGO thickness, but the stress magnitude at the early cycles increases due to additional thermal mismatch. The sintering does affect the stress magnitude at the latter thermal cycles. The method can be further implemented in other geometry with different crack locations, orientations, or number of cracks to estimate the crack propagation life.

8.2.1 REFERENCES

[18] Miehe, Christian, Martina Hofacker, and Fabian Welschinger. "A phase field model for rate-independent crack propagation: Robust algorithmic implementation based on operator splits." Computer Methods in Applied Mechanics and Engineering 199, no. 45-48 (2010): 2765-2778.
DOI: 10.1016/J.CMA.2010.04.011.

9.0 ACKNOWLEDGEMENTS

The NRC Aerospace project on Technology Watch for Defense & Civil Dual-Use, under the Aerospace Focused Area, "*Defence Platform and Sustainment (DPS)*", provided support for NRC's effort to prepare for this ICAF National Review.

Special thanks to all the organizations and authors who have contributed various inputs to the Canadian National Review for ICAF 2025.

Special thanks to Dr. Guillaume Renaud for reviewing this report.